博士論文

The study of pre-rRNA accumulation under nutrient deprivation in cancer cells
(飢餓状態のがん細胞におけるpre-rRNA蓄積に関する研究)

パン メルビン

Table of contents

Abbreviations

5-Fluorouridine (5FU)

Aberrant crypt foci (ACF)

AMP-activated protein kinase (AMPK)

double-stranded RNA-dependent protein kinase (PKR)

eIF4E-binding protein 1 (4E-BP1)

endoplasmic reticulum (ER)

eukaryotic elongation factor 2 (eEF2)

eukaryotic elongation factor 2 kinase (eEF2K)

Eukaryotic translation initiation factor 4E (eIF4E)

general control non-derepressible 2 (GCN2)

Glutamine (Gln)

heme-regulated eIF2α kinase (HRI)

hepatitis B virus (HBV)

hepatitis C viruses (HCV)

human papilloma virus (HPV)

hypoxia-inducible factor 1α (HIF1α)

Integrated stress response (ISR)

integrated stress response (ISR)

mammalian target of rapamycin complex 1 (mTORC1)

medical linear accelerator (LINAC)

murine double minute gene 2 (MDM2)

Nutrient deprivation (ND)

Nutrient restoration (NR)

PKR-like ER kinase (PERK)

Precursor ribosomal RNA (pre-rRNA)

prolyl hydroxylases (PHD)

ribosomal DNA (rDNA)

Ribosomal proteins (r-proteins)

RNA Polymerase I (Pol I)

transcription initiation factor IA (TIF-IA)

von Hippel-Lindau tumor suppressor (pVHL)

Abstract of Dissertation

Malignant growth depends on protein synthesis and is therefore reliant on the production of ribosomes. Ribosome biogenesis starts in the nucleolus where RNA Polymerase I (Pol I) synthesizes the precursor ribosomal RNA (pre-rRNA). Perturbations in ribosome biogenesis activate p53 through the nucleolar surveillance pathway. Mechanisms employed by tumor cells to escape p53 nucleolar surveillance remain unidentified. Here, we show that nutrient deprived cells in solid tumors accumulate pre-RNAs to suppress p53 during metabolic recovery. Nutrient deprived cells accumulate pre-rRNAs by severely slowing pre-rRNA processing. Upon nutrient restoration, metabolically recovering cells resume ribosome biogenesis and accumulated pre-rRNAs are bound by the ribosomal proteins uL5 (formerly termed RPL11) and uL18 (RPL5). Inhibiting pre-rRNA accumulation results in newly synthesized uL5 and uL18 binding to MDM2 during metabolic recovery, leading to nutrient-induced p53-mediated apoptosis. We identify glutamine as the key nutrient that promotes the de novo protein synthesis of uL5 and uL18. Mechanistically, glutamine activates Ras/Raf/MEK/ERK signalling, which promotes uL5/uL18 synthesis through stimulating mammalian target of rapamycin complex 1 (mTORC1) and the eukaryotic elongation factor 2 (eEF2). Pharmacologically inhibiting Raf/MEK/ERK inhibits the synthesis of uL5 and uL18 and abrogates the stabilization of p53. Depriving cancer cells of glutamine blocks the p53 nucleolar surveillance pathway, thus hampering the therapeutic response to Pol I inhibitors. Our data reveals an adaptive mechanism that tumor cells exploit to suppress p53 during fluctuations in environmental nutrient availability.

Keywords

Nucleolar stress response, p53, nutrient deprivation, RNA Polymerase I, pre-rRNA processing, tumor microenvironment

Chapter One: Introduction

The Cancer Problem

Normal cells are transformed into cancerous cells through the sequential accumulation of mutations to the genome. Damage that occurs to the genome can occur from internal processes and external assaults (Bertram, 2000). Most of the resulting mutations are patched by a collection of DNA repair processes, but unrepaired mutations in crucial tumor suppressor or oncogenes can result in cell transformation (Zheng et al., 2000). These crucial genes generally control cellular mechanisms involved in cell proliferation and cell death (Chiarugi et al.). Malignant cancers share six hallmarks: sustaining cell proliferation, escaping growth suppression, activating invasion and metastatic processes, overcoming replicative senescence, resisting cell death, and inducing angiogenesis (Hanahan and Weinberg, 2011).

Treating Cancer

Cancer treatments mainly involve chemotherapy, surgery, radiotherapy, and immunotherapy (*i.e.* oncolytic viruses). During World War I and II, it was observed that soldiers that were exposed to mustard gas possessed lower levels of white blood cells, and this led to nitrogen mustard being used as the first chemotherapeutic agent against a variety of blood cancers (Hodgkin's disease, lymphosarcoma, leukemia) (Goodman and Wintrobe, 1946). In 1957, 5-fluorouracil was developed as a treatment for solid tumors, which is currently being used today against colorectal, head and neck cancers (Heidelberger et al., 1957).

In the 1960s, surgery and radiotherapy was often the main choice for solid tumor treatments. Surgery involves the removal of the primary solid tumor. Radiotherapy involves the delivery of high-energy x-rays or electrons to the patient tumor by a medical linear accelerator (LINAC), which is a device that is commonly used for radiation treatment. Radiotherapy can be given before surgery to reduce the tumor mass, or can be used as the main treatment method for hard-to-reach tumors. Tumor cells that are subject to radiotherapy undergo DNA single- and double-strand breaks that results in cell apoptosis. Despite the initial effectiveness of surgery and radiotherapy, cure rates were strongly hindered by the inability to eliminate micrometastases. Thus, surgery/radiotherapy treatment was followed by adjuvant chemotherapy to eliminate remaining tumor cells (Arruebo et al., 2011).

Immunotherapy uses antibodies, cytokines, and dendritic cells to treat cancers. Antibodies, which are produced by B-cells, can provide specificity and lower toxic side effects when compared to surgery, chemotherapy, and radiotherapy. The first use of antibodies as a cancer treatment was in 1982, where antibodies that bind to the surface immunoglobulin of malignant B cells was successfully used against B-cell lymphoma (Miller et al., 1982). To date, over 230 antibodies have entered clinical trials for various diseases (Arruebo et al., 2011).

Colorectal cancer epidemiology and pathogenesis

Colorectal cancer is the third most commonly diagnosed cancer in men and second most in women (Bray et al., 2018). Worldwide, it accounts for ~10% of diagnosed cancer cases and cancer-related deaths (Yang et al., 2020). It is projected that worldwide cases will increase to 2-5 million new cases per year by 2035 (Arnold et

al., 2017; Bray et al., 2018). Disease screening programmes and the increased use of colonoscopy has been attributed to the stabilization of new cases in developed countries (Ait Ouakrim et al., 2015).

Most colorectal cancer cases begin from a precancerous lesion termed Aberrant crypt foci (ACF) that evolves into a neoplastic precursor lesion (*i.e.* polyp), which eventually progresses into colorectal cancer, and this transformation is estimated to take 10-15 years (Kowalczyk et al., 2018). It is generally thought that colorectal cancers develop from a stem cell or stem-cell like cell, and cancer stem cells are located in the base of colonic crypts, and are critical for tumor initiation (Medema, 2013). There are two major tumor initiation pathways: the adenoma-carcinoma pathway accounts for 70-90% of colorectal cancer cases, and the serrated neoplasia pathway accounts for 10-20% of cases (Arnold et al., 2017; Bray et al., 2018). The adenoma-carcinoma pathway typically develops from an *APC* mutation, and *Ras* and *TP53* mutations follow afterwards (Dekker et al., 2019). The serrated neoplasia pathway is characterized by *RAS/RAF* mutations and epigenetic instability (Dekker et al., 2019). Further, colorectal cancer can be left-sided (distal) or right-sided (proximal), and left/right sidedness plays a key role in metastatic outcome and response to drugs that target EGFR (Loree et al., 2018).

Induction of angiogenesis as a hallmark of cancer

The ability to induce angiogenesis is considered to be one of the six hallmarks of cancer (Hanahan and Weinberg, 2011). Solid tumors outstrip their blood supply and develop tissue microenvironments that are depleted of oxygen and nutrients (El-Naggar et al., 2015; Leprivier et al., 2013). Such microenvironments are

characterized by chronic hypoxia and are typically located more than 180 μm away from blood vessels (Dewhirst, 2018; Thomlinson and Gray, 1955). The severity of pathologic hypoxia varies between tumor types, but it is generally thought that hypoxic tissue contains 1-2% O_2. Indeed, as the distance between the blood vessel and tumor cell increases, the oxygen levels decrease. Notably, the concentration of oxygen in normal tissues ranges between ~9.5% O_2 for the renal cortex and ~4.5% $O_2$for the brain, further, cell culture experiments are performed with atmospheric levels of oxygen (21% O_2), meaning that experimental conditions are performed in 'hyperoxic' conditions rather than physiological conditions (Muz et al., 2015). The most well known adaptation to hypoxia is the induction of hypoxia-inducible factor 1α (HIF1α), a heterodimeric transcription stabilized by low oxygen that transactivates genes involved in glycolysis, angiogenesis, and metastasis (Semenza, 2003). Under oxygen-rich conditions, HIF1α is constitutively degraded through the proteasomal pathway, and this pathway is promoted by by von Hippel-Lindau tumor suppressor (pVHL) protein, which is an E3 ubiquitin ligase that ubiquitinates HIF1α (Kamura et al., 1999). In order for pVHL to recognize and bind to HIF1α, HIF1α must be hydroxylated by prolyl hydroxylases (PHD), which uses oxygen as a co-substrate (Ohh et al., 2000). Upon hypoxia, PHDs become inhibited, and HIF1α becomes stabilized due to reduced hydroxylation (Ivan et al., 2001). HIF1α activates a transcriptional program of >60 genes involved in angiogenesis (*i.e.* VEGF), cell proliferation, cell survival, glucose metabolism, and iron metabolism (Semenza, 2003). The key role of HIF1α in tumor progression has attracted considerable attention in targeting its transcriptional activity as a therapeutic. Another type of hypoxia— known as 'cycling hypoxia' — arises from transient shutdown of immature

vasculature (Harris, 2002; Kimura et al., 1996).

Nutrient deprivation in the solid tumor microenvironment

Along with hypoxia, unstable blood supply also causes substantial fluctuations in nutrient availability in the tumor microenvironment (Jones and Thompson, 2009). Nutrient deprivation severely inhibits tumor cell proliferation but selects for aggressive cells that display increased angiogenic and metastatic ability (Osawa and Shibuya, 2013; Pàez-Ribes et al., 2009). In order to preserve energy balance during metabolic stress, tumor cells evolve adaptive mechanisms to attenuate ATP-costly processes under nutrient deprivation (Silvera et al., 2010).

Molecular adaptations to nutrient deprivation involve the inhibition of protein synthesis, which is the most energy consuming process in the cell (Buttgereit and Brand, 1995). Further, most of these adaptive mechanisms focus on inhibiting the initiation and elongation steps of translation. For instance, the eukaryotic elongation factor 2 kinase (eEF2K) responds to nutrient restriction by inhibiting the eukaryotic elongation factor 2 (eEF2) (Leprivier et al., 2013). eEF2 facilitates the GTP-dependent translocation step of the nascent peptide from the A-site to the P-site of the ribosome (Leprivier et al., 2013). Thus, eEF2K phosphorylates and inactivates eEF2 to promote cell survival under nutrient depletion (Leprivier et al., 2013). Metabolic stress inhibits mammalian target of rapamycin complex 1 (mTORC1) (Liu and Sabatini, 2020). This impairs mRNA translation initiation by activation of the eIF4E-binding protein 1 (4E-BP1), which inhibits the cap-binding translation initiation factor Eukaryotic translation initiation factor 4E (eIF4E) (Liu and Sabatini, 2020). In addition to nutrient stress, the ISR is activated in response to

diverse stress stimuli, such as hypoxia, viral infection, and endoplasmic reticulum (ER) stress (Costa-Mattioli and Walter, 2020). Notably, the phosphorylation of eIF2α by the ISR is controlled by four conserved kinases: PKR-like ER kinase (PERK), double-stranded RNA-dependent protein kinase (PKR), heme-regulated eIF2α kinase (HRI), and general control non-derepressible 2 (GCN2) (Costa-Mattioli and Walter, 2020). Another critical adaptation is the suppression of rRNA synthesis by RNA Polymerase I (Pol I), which normally makes up 60% of total cellular transcription (Hoppe et al., 2009; Mayer, 2004). mTORC1 and AMP-activated protein kinase (AMPK) reciprocally regulate pre-rRNA biosynthesis by phosphorylating transcription initiation factor IA (TIF-IA), the protein complex that anchors Pol I to the rDNA promoter (Hoppe et al., 2009; Mayer, 2004). While oncogenic adaptations to nutrient deprivation have been well characterized, it is unknown how starving tumor cells resume proliferative capacities upon nutrient restoration.

The tumor suppressor p53

The p53 protein was first identified through its interaction with SV40 large T antigen (May and May, 1999). In unstressed cells, wildtype p53 is constitutively degraded via the proteasome, and this process is facilitated by murine double minute gene 2 (MDM2) (HDM2 in humans, henceforth denoted MDM2) (Levine, 2020). Upon DNA damage, MDM2 becomes phosphorylated in an ATM-dependent manner and its E3 ligase activity towards p53 becomes inhibited, and this leads to p53 stabilization (Lavin and Gueven, 2006). Upon the stabilization of the p53 protein, the N-terminus of p53 becomes post-translationally modified (*i.e.* phosphorylation, acetylation, methylation, ubiquitination, and sumoylation) (Lavin and Gueven, 2006). Further,

other stresses such as hypoxia and replicative stress have been demonstrated to activate p53 (**Figure 1.1**). Following activation, p53 activates genes involved in apoptosis, growth arrest, senescence, and DNA repair (**Figure 1.1**). For instance, p53 activates p21 to induce growth arrest, but can also transcriptionally activate Puma to induce Puma-dependent apoptosis (Sperka et al., 2011).

Ribosome biogenesis and the nucleolar surveillance pathway

Ribosomes translate mRNAs into functional proteins and are one of the fundamental molecular machines to life. Given the role of ribosomes in cellular growth, it is not surprising that elevated ribosome biogenesis has been shown to play critical roles in tumor initiation and growth (Pelletier et al., 2018). Ribosome biogenesis starts in the nucleolus where Pol I synthesizes a long polycistronic pre-rRNA that undergoes rapid folding, modification, and processing, and associations with r-proteins (**Figure 1.2**) (Lafontaine, 2015). In the nucleolus, Pol I transcribes several hundred ribosomal DNA (rDNA) (Lafontaine, 2015). Maturation of the pre-rRNA produces the 18S, 5.8S, and 28S rRNAs (Lafontaine, 2015). By contrast, the 5S rRNA (several hundred copies) gene is located outside the nucleolus and is transcribed by RNA Polymerase III. Thus, ribosome biogenesis requires the coordinated efforts of RNA Pol I, II, and III.

Inhibiting ribosome biogenesis potently destroys nucleolar integrity and leads to the activation of p53. This observation was first reported by Pestov *et al*., where inhibiting the nucleolar Bop1 protein could inhibit ribosome biogenesis and stabilize p53 (Pestov et al., 2001). Since ribosome biogenesis mainly occurs in the nucleolus, the activation of p53 by this regulatory loop is known as the ‘nucleolar surveillance

pathway'. Actinomycin D, which potently inhibits global transcription, is the most commonly used chemotherapeutic to induce nucleolar stress (Pestov et al., 2001). However, the most specific way of inducing nucleolar stress is by specifically targeting RNA polymerase I with first-in-class inhibitors such as CX-5461 and BMH-21 (**Figure 1.3**) (Bywater et al., 2012; Peltonen et al., 2014). When ribosome biogenesis is compromised, ribosomal components accumulate freely in cells, including the r-proteins uL5 (formerly known as RPL11) and uL18 (RPL5), which, together with the 5S rRNA, form a stable trimeric complex that binds and inhibits MDM2, leading to p53 stabilization and subsequent p53-mediated cell cycle arrest or apoptosis (**Figure 1.4**) (Donati et al., 2013; Nicolas et al., 2016; Sloan et al., 2013). To note, p53 is canonically induced by DNA damage (genotoxic chemicals, IR irradiation). The stabilization of p53 by DNA damage does not require uL5/uL18, and uL5/uL18 is only required for the activation of p53 via the nucleolar surveillance pathway. Distinct pathways that activate p53 require different-activating molecules. For instance, genotoxic activation of p53 requires the ATM kinase (Banin, 1998), and oncogene-mediated activation of p53 requires the tumor suppressor ARF(Sherr, 2006).

The importance of Nutrients to Cancer Growth

Cancer cells must rapidly uptake nutrients in order to rapidly divide. Glucose and glutamine are the two key nutrients that support oncogenic growth. Glucose is metabolized via glycolysis and the pentose phosphate pathway to produce pyruvate, ATP, ribose 5-phosphate, and NADPH. Deprivation of glucose can cause cell death. Increased glucose consumption was first described by Warburg (Warburg, 1956). In

the 1950s, Warburg observed that cancer cells consume ten times more glucose than non-dividing cells, and that consumed glucose was converted to lactate ("Warburg effect") (Warburg, 1956). The importance of glutamine was first described by Eagle in 1955 (Eagle, 1955). Eagle observed that HeLa cells consumed 10-100 times more glutamine than other amino acids (Eagle, 1955). Glutamine is consumed through the tricarboxylic acid (TCA) cycle to generate ATP and precursors for nucleotides and lipids (Altman et al., 2016). The contribution of other amino acids such as Asparagine (non-essential) and leucine (essential) has been studied in cancer metabolism. For instance, asparagine is required to maintain the viability of acute lymphoblastic leukemia cells (Clavell et al., 1986). Targeting asparaginase (the enzyme which metabolizes asparagine) has been approved for treating acute lymphoblastic leukemia. Similarly, leucine is required to maintain the viability of melanoma cells due to defective autophagy (Sheen et al., 2011).

Aim

It is well known that tumor cells experience fluxes in nutrient availability in the solid tumor microenvironment. Further, the synthesis of rRNAs and r-proteins is tightly coordinated with nutrient availability, and perturbations in ribosomal assembly activates the p53-dependent nucleolar surveillance pathway. However, it is not clear how metabolically recovering cancer cells resume ribosome biogenesis, *i.e.* when starving cells are subject to nutrient stress termination. In this study, we first aim (Chapter 2) to understand how pre-rRNA synthesis and processing is affected by nutrient deprivation. As outlined in chapter 3, we later studied the consequences of perturbed pre-rRNA metabolism under nutrient deprivation, and its lethal effects

during nutrient restoration. Finally, chapter 4 studies the effects of nutrient deprivation, specifically glutamine deprivation, on the p53-dependent nucleolar surveillance pathway.

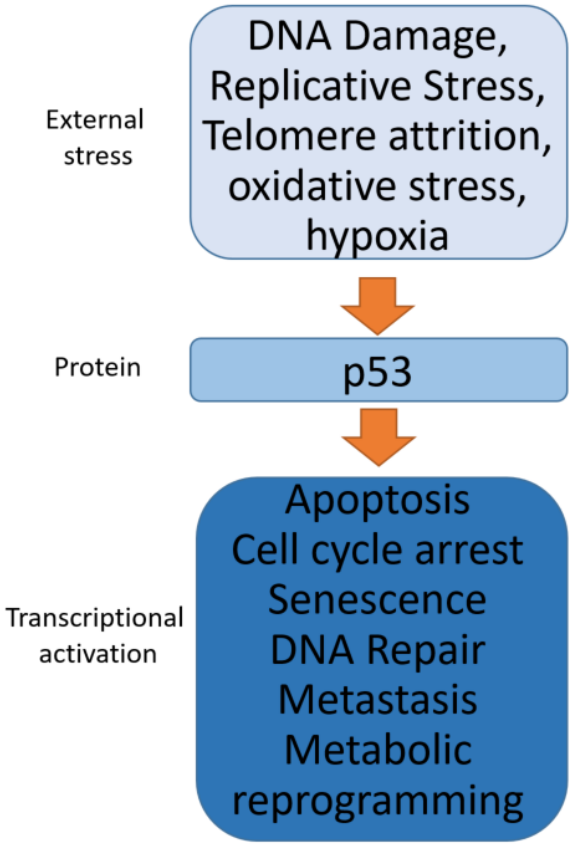

Figure 1.1: p53 is activated by a variety of stresses. Subsequent activation of p53 results in tumor suppression by activation of genes involved in cell cycle arrest, senescence, and apoptosis.

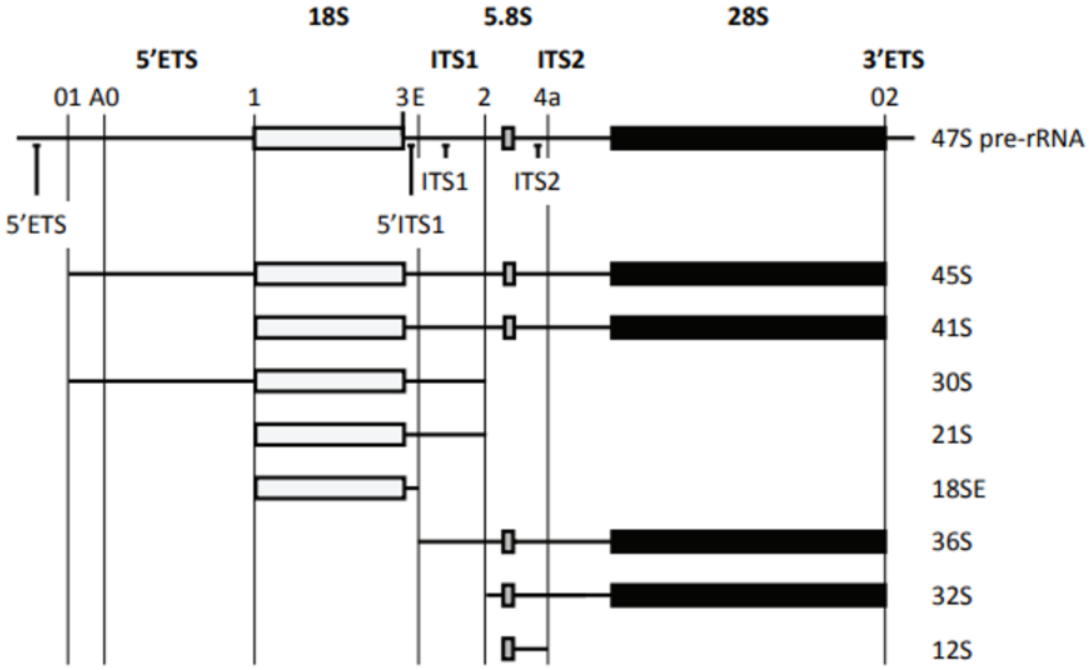

Figure 1.2 Pre-rRNA processing in human cells. 47S processing produces intermediate precursors which mature to 18S, 28S, and 5.8S rRNAs. The primary 47S pre-rRNA contains two external transcribed spacers (5'ETS and 3'ETS) and two internal transcriber spacers (ITS1 and ITS2). Processing at each external/internal spacer occurs at specific cleavage sites. The 5'ETS contains three cleavage sites: 01 and A0 are located within the 5'ETS and site 1 is located at the 5' end of the 18S rRNA.

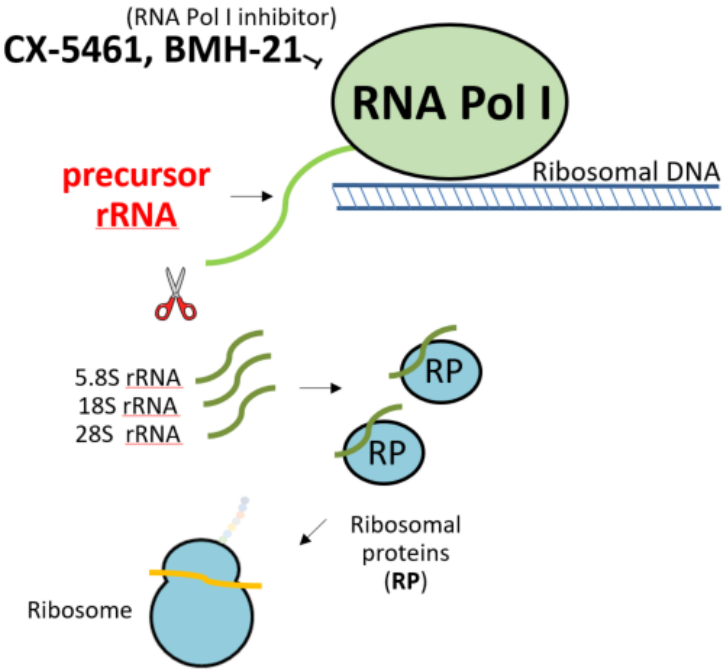

Figure 1.3: CX-5461 and BMH-21 inhibit rDNA transcription through different mechanisms. (A) CX-5461 blocks SL1 from binding to Pol I, which prevents Pol I from binding to rDNA. (B) BMH-21 is a DNA intercalator which binds to rDNA, preventing Pol I transcription elongation.

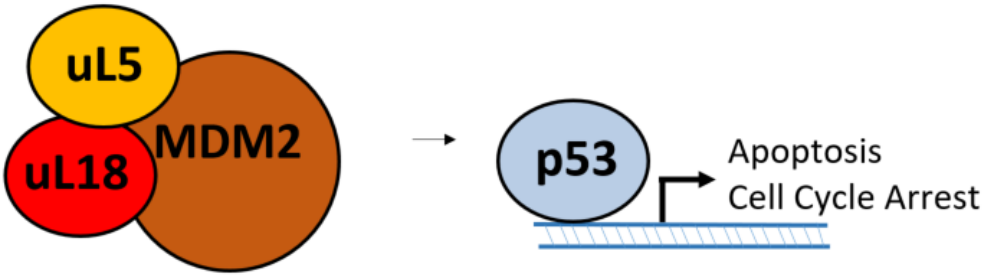

Figure 1.4: During nucleolar stress (such as CX-5461 or BMH-21 treatment), ribosomal proteins freely accumulate in stressed cells. Further, accumulated uL5 and uL18 form a trimeric complex with the 5S rRNA (not shown) to bind and inhibit MDM2. Upon MDM2 inhibition, p53 becomes stabilized.

Chapter Two: HCT116 cells accumulate pre-rRNAs under nutrient deprivation by slowing pre-rRNA processing

Background and significance

Malignant growth depends on protein synthesis and is therefore reliant on the production of ribosomes. A key mediator is RNA Polymerase I, which transcribes ribosomal DNA in nucleoli to produce a polycistronic precursor rRNA (**pre-rRNA**) that is processed to generate the 18S, 5.8S, and 28S rRNAs that form the ribosome core (Pelletier et al., 2018). Cancer cells with high cell growth display elevated rDNA transcription compared to nontransformed cells, and consequently, enlarged nucleoli have been used as prognostic marker of aggressive malignancies (Derenzini et al., 2009). Inactivating mutations in tumor suppressors that negatively regulate Pol I, including p53, Rb, and ARF, further deregulate rRNA synthesis and promote cell growth (Pelletier et al., 2018).

The first selective inhibitor of Pol I was discovered in 2009, named CX-3543, and acts by disrupting G-quadruplex structures found in rDNA and thereby inhibiting Pol I transcription (Drygin et al., 2009). Other Pol I inhibitors that were subsequently discovered included CX-5461 and BMH-21, which are being investigated as anticancer compounds (Fig 1.2) (Khot et al., 2019; Peltonen et al., 2014). CX-5461 targets the Pol I pre-initiation complex by interfering with SL1 recognition of the ribosomal DNA promoter (Drygin et al., 2011). BMH-21 stops Pol I transcriptional elongation by intercalating with ribosomal DNA, causing the proteasomal degradation of the Pol I component RPA194 (Scull and Schneider, 2019). Pol I inhibition by CX-5461 or BMH-21 subsequently activates p53 through the nucleolar

stress response pathway (Holmberg Olausson et al., 2012; Sloan et al., 2013). Reduction of pre-rRNA by CX-5461 or BMH-21 causes unassembled ribosomal proteins (uL5 and uL18) to accumulate and bind to MDM2, inhibiting the E3 ubiquitin ligase activity of MDM2 to p53 and stabilizing p53 (Bywater et al., 2012; Peltonen et al., 2014). The ribosomal proteins uL5 and uL18 form a complex with 5.8S rRNA before binding to MDM2 (Holmberg Olausson et al., 2012; Sloan et al., 2013).

Pre-rRNA processing is a highly orchestrated pathway that requires at least 300 factors and involves a strict sequence of nucleotide modifications, cleavages, and associations with ribosomal proteins (RPs) (Mullineux and Lafontaine, 2012). It is well known that cells suppress rDNA transcription by Pol I under nutrient stress to conserve energy, but it is unknown how pre-rRNA processing is affected by nutrient stress. Thus, initial experiments were performed to determine the effect of nutrient deprivation on pre-rRNA processing.

Methods

Cell lines and Reagents

HCT116, A375, A549, U2OS, and MKN45, cells were purchased from the American Type Culture Collection (Manassas, VA, USA). HCT116 p53+/+ and p53−/− isogenic human colon cancer cells were kindly provided by Bert Vogelstein (Johns Hopkins University). HCT116, A375, A549, and U2OS cells were grown in Dulbecco's modified Eagle's medium (DMEM) (Nacalai Tesque, Kyoto, Japan), supplemented with 10% fetal bovine serum (FBS) (Thermo Fisher Scientific). MKN45 cells were maintained in RPMI (Nacalai Tesque, Kyoto, Japan), supplemented with 10% FBS. Cells were maintained at 37C in a 5% CO2 atmosphere in a humidified incubator. Nutrient deprivation medium was prepared to contain inorganic salts, i.e., 0.2 g/l CaCl2 (anhydrous), 0.1 mg/l Fe(NO3)3/9H2O, 0.4 g/l KCl, 97.67 mg/l MgSO4 (anhyd.), 6.4 g/l NaCl, 3.7 g/l NaHCO3, 0.125 g/l NaH2PO4/H2O, and 15 mg/l Phenol Red, according to the composition of DMEM.

5-Fluorouridine Metabolic Labelling and Microscopy

To measure pre-rRNA biosynthesis, cells were seeded at 50% confluence in 6-well plates containing round cover glasses (12CIR-1D; Thermo Fisher Scientific). After treatment, cells were incubated with 10 μM 5-Fluorouridine (5FU) (TCI chemicals) for 3 h, followed by fixation with methanol at -20°C for 30 min and blocking with milk (5% in PBS). 5FU was visualized using primary BrdU antibody (1:500 Sigma Aldrich) and the nucleolus was visualized by staining for nucleolin (1:1000 Cell signaling technology). Detection of primary antibodies was performed with Alexa Fluor 488 Goat anti-Mouse IgG (1:2000 Thermo Fisher Scientific) and Alexa Fluor 594 Goat

anti-Rabbit IgG (1:2000 Thermo Fisher Scientific). Slides were mounted with Prolong Gold Antifade Mountant with DAPI (Thermo Fisher Scientific) and viewed using BZ-X710 fluorescence microscope or LSM700 confocal microscope (CLSM, Carl Zeiss, Jena, Germany). For 5FU fluorescence quantification, three images were taken at random per treatment with a 100× objective lens and signal intensity was quantified from using ImageJ software. 5FU intensity for each image was divided by the number of cells and fold change was calculated by setting the control cells to one.

RNA Isolation and quantitative RT-PCR

Total RNA was extracted from cells using the Isogen reagent (Nippon Gene, Toyama, Japan), converted to cDNA by using the Prime Script reverse transcriptase (Takara, Shiga, Japan) as per the manufacturer's instructions, and used for quantitative real-time PCR amplification using SYBR Green (Takara). Target RNA expression was normalized to β2m mRNA.

The following primer sequences were used:

For pre-rRNA expression:

5′-CCGCGCTCTACCTTACCTACCT-3'(forward);

5′-GCATGGCTTAATCTTTGAGACAAG-3′(reverse).

For human β2m:

5′-AGATGAGTATGCCTGCCGTG-3′;

5′-CATCCAATCCAAATGCGGCA-3′.

Cell line xenograft murine model

All animal care procedures were in accordance with institutional guidelines approved by the University of Tokyo. HCT116 cells (5 × 106 in 100 μL PBS) were inoculated subcutaneously in the right flank of nude mice. After treatments, animals were euthanized, and tumors were harvested for further analysis.

Results

Cancer cells accumulate pre-rRNAs under nutrient deprivation by slowing pre-rRNA processing

We cultured a broad range of solid tumor cell lines (colorectal HCT116, melanoma A375, lung adenocarcinoma A549, osteosarcoma U2OS, gastric MKN45) in nutrient deprivation (**ND**) media for 24 h (-glucose, -amino acids, -FBS) and measured Pol I transcriptional activity by labelling nascent pre-rRNAs with 5-fluorouridine (**5FU**). In all cell lines tested, ND strongly suppressed Pol I, but, surprisingly, basal levels of pre-rRNA synthesis persisted even after the prolonged withdrawal of all critical nutrients (**Fig 2.1**). This suggested that pre-rRNA expression may be important to ND, so we measured pre-rRNA levels in control and ND cells using qRT-PCR. We used primers that recognize sequences flanking site 01 of the 5'-external transcribed sequence (5'ETS) of the pre-rRNA, which measures the total abundance of the 47S, 45S, and 30S pre-rRNAs (**Fig 2.2**). Unexpectedly, despite lowered pre-rRNA synthesis, ND strongly elevated pre-rRNA expression in HCT116, A549, U2OS, and MKN45 cells (**Fig 2.3**). Thus, cancer cells upregulate pre-rRNA expression under ND.

We hypothesized that HCT116 cells accumulate pre-rRNA by slowing pre-rRNA processing under ND. To investigate this, we measured the RNA half-life of the pre-rRNAs (47S, 45S, 30S) in control and ND HCT116 cells. Transcription was halted with actinomycin D, a potent inhibitor of Pol I, and pre-rRNA turnover kinetics were monitored over one hour. Pre-rRNA levels precipitously dropped after transcriptional inhibition under control conditions while turnover was severely slowed under ND (**Fig 2.4**). Consequently, the pre-rRNA half-life was greatly extended under

ND: control λ = 28 min, ND λ = 78 min (**Fig 2.4**). In conclusion, mammalian cells accumulate pre-rRNAs under ND by slowing pre-rRNA processing.

Solid tumors with abnormal vasculature contain microenvironments that are strongly deprived of nutrients (Jones and Thompson, 2009), implying that *in vivo* ND should similarly slow down tumor cell pre-rRNA processing. To investigate this, HCT116 tumors were directly injected with actinomycin D and pre-rRNA turnover kinetics were monitored. Since the cores of tumors are more severely depleted of nutrients compared to the periphery (Pan et al., 2016), we reasoned that core tumor cells would display higher pre-rRNA levels and slower pre-rRNA processing kinetics than periphery cells. Thus, intratumoral injection of actinomycin D was followed by dissection of tumors in peripheral vs. core tissues to differentiate tumor cells under high or low nutrient conditions, respectively (Pan et al., 2016). In line with our *in vitro* observations, core tissues had higher levels of pre-rRNAs than the periphery (**Fig 2.5**). Core tissues expressed higher HIF1α levels than peripheral tissues, consistent with the notion that core regions are avascular (**Fig 2.6**). Further, peripheral pre-rRNA exhibited a half-life of 120 minutes while core pre-rRNA displayed greater stability, with no decrease in pre-rRNA abundance after 120 min of transcriptional inhibition (**Fig 2.7**). Finally, 3T3-L1 MEFs also accumulated high levels of pre-rRNAs under ND, showing that pre-rRNA accumulation is a phenomenon that is conserved among mammalian cells (**Fig 2.8**). In conclusion, nutrient deprived cells in tumor cores accumulate pre-rRNAs by slowing pre-rRNA processing.

Slowed pre-rRNA processing in solid tumors diminishes CX-5461 on-target drug activity

CX-5461 and BMH-21 are Pol I inhibitors that inhibit ribosome biogenesis by blocking pre-rRNA synthesis (Bywater et al., 2012; Peltonen et al., 2014). The most robust and quantitative method for measuring on-target drug activity against Pol I is by monitoring pre-rRNA expression by qRT-PCR. Due to the short half-life of the pre-rRNA (~30 min), Pol I inhibitors are capable of acutely decreasing pre-rRNA expression within 1 h of treatment *in vitro* (**Fig 2.9**) (Bywater et al., 2012; Peltonen et al., 2014). However, since we found that pre-rRNAs possess extended half-lives under ND, this predicts that Pol I inhibitors would be less capable of acutely decreasing the stabilized pre-rRNAs under ND (**Fig 2.9**). To demonstrate this, we exposed control or ND HCT116 cells to CX-5461 (0, 1, 5, 10 μM) for 8 h. As expected, under control conditions, CX-5461 (1 μM) strongly decreased pre-rRNA expression by 50% (**Fig 2.10**). However, under ND, the same concentration (1 μM) failed to affect pre-rRNA expression (**Fig 2.10**). Furthermore, a higher concentration of CX-5461 (10 μM) was needed to successfully inhibit pre-rRNA (**Fig 2.10**). Notably, CX-5461 has been shown to induce DNA damage at this concentration (Xu et al., 2017). We quantified this effect and found that CX-5461 inhibited pre-rRNA at an IC50 of 1 μM under control conditions whereas the IC50 was 6.4 μM under ND (**Fig 2.11**). BMH-21, a second Pol I inhibitor, also failed to inhibit pre-rRNA expression under ND when treated at 0.1 μM, indicating the need for a high dose to inhibit pre-rRNA Expression under ND (**Fig 2.12**). These results show Pol I inhibitors display reduced on-target drug activity against nutrient stressed cells that process pre-rRNAs slowly. Next, since *in vivo* cells display severely slowed pre-rRNA processing, we predicted that CX-5461 would fail to acutely deplete tumoral pre-rRNA expression. Indeed, intraperitoneal (IP) injection of CX-5461 failed to

inhibit pre-rRNA expression in HCT116 tumors (**Fig 2.12**). Together, these results show that *in vivo* ND diminishes the on-target drug activity of Pol I inhibitors by stabilizing the pre-rRNA molecule.

Discussion

It is generally thought that mammalian cells inhibit energy consuming anabolic processes under nutrient stress and divert energy towards catabolic processes that maintain intracellular ATP homeostasis. For instance, it is known that human cells inhibit global protein synthesis under nutrient depletion by activating eEF2K and inhibiting mTORC1 and eIF2α (Leprivier et al., 2013). Despite this, we first observed that a broad range of human cancer cell lines (colorectal HCT116, melanoma A375, lung adenocarcinoma A549, osteosarcoma U2OS, gastric MKN45) preserve rDNA transcription by Pol I under the prolonged ND (24 h). We subsequently found that basal Pol I activity was part of a larger cellular effort to accumulate pre-rRNAs under nutrient depletion. The second half of the effort involved stabilizing pre-rRNA by slowing precursor processing. Slowed processing was similarly observed in animal models, where *in vivo* tumor cells possess pre-rRNAs with longer half-lives than cells *in vitro* (in vitro: 28 minutes, in vivo: 120 minutes). We conclude that tumor cell populations have heterogeneous processing speeds, dependent on nutrient availability. This situation poses a problem to Pol I inhibitors, which rely on fast processing speeds to acutely decrease precursor levels. Indeed, under full nutrient conditions, where the pre-rRNAs are unstable, Pol I inhibition by CX-5461 acutely depletes endogenous pre-rRNA expression. However, under ND, CX-5461 failed to inhibit pre-rRNA expression. Accordingly, IP injection with CX-5461 failed to inhibit pre-rRNA expression in HCT116 tumors, showing that Pol I inhibitors display diminished drug activity in solid tumors due to *in vivo* ND. These results suggest that application of Pol I inhibitors to solid tumors may be hindered by slowed pre-rRNA processing in vivo. Together, these results show that cancer cells slow pre-rRNA

processing to accumulate pre-rRNAs. Thus, the next chapter is dedicated to studying why pre-rRNA accumulation is important to metabolic stress.

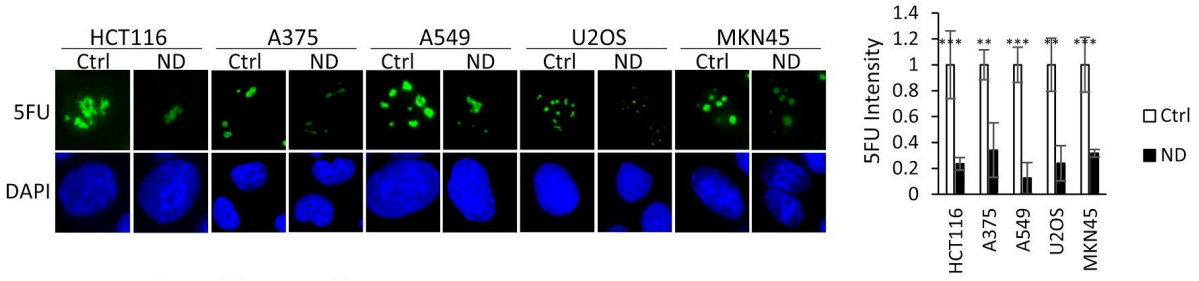

Figure 2.1: Cancer cell lines preserve basal Pol I activity under long term ND (24 h). Cancer cell lines were cultured under ND for 24 h, and pre-rRNA biosynthesis was measured by 5FU metabolic labelling.

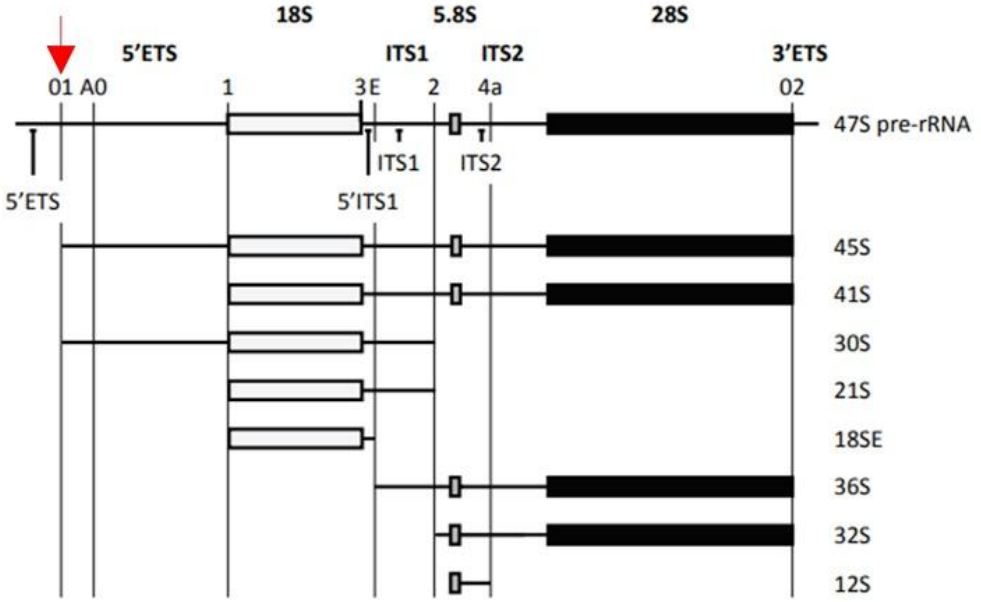

Figure 2.2: Schematic of pre-rRNA processing. 47S processing produces intermediate precursors which mature to 18S, 28S, and 5.8S rRNAs. The primary 47S pre-rRNA contains two external transcribed spacers (5'ETS and 3'ETS) and two internal transcriber spacers (ITS1 and ITS2). The red arrow shows the binding site of the human pre-rRNA primers for qRT-PCR.

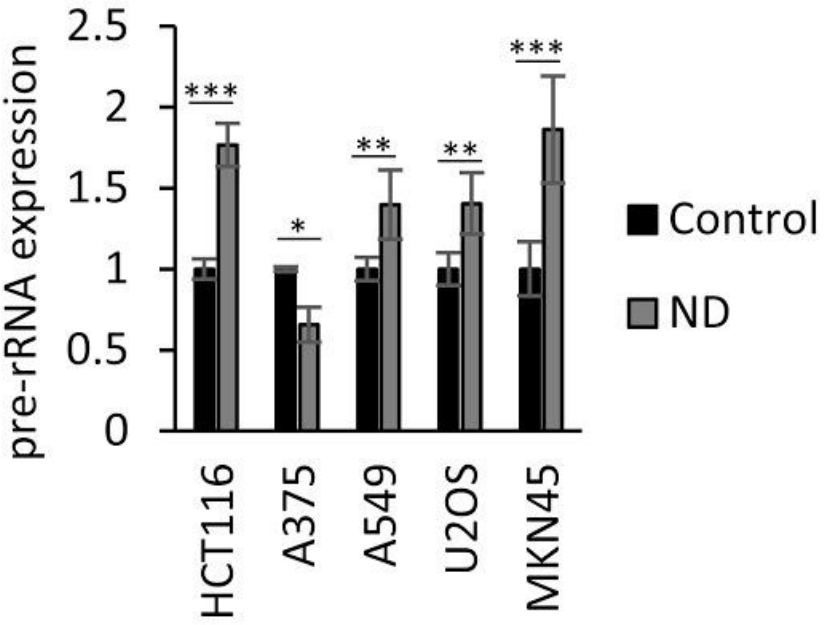

Figure 2.3: ND (24 h) increases pre-rRNA expression (47S, 45S, 30S) in HCT116, A549, U2OS, and MKN45 cells but not A375 as assessed using qRT-PCR. Cells were cultured to ND for 24 h and RNA was isolated for pre-rRNA expression analysis via qRT-PCR.

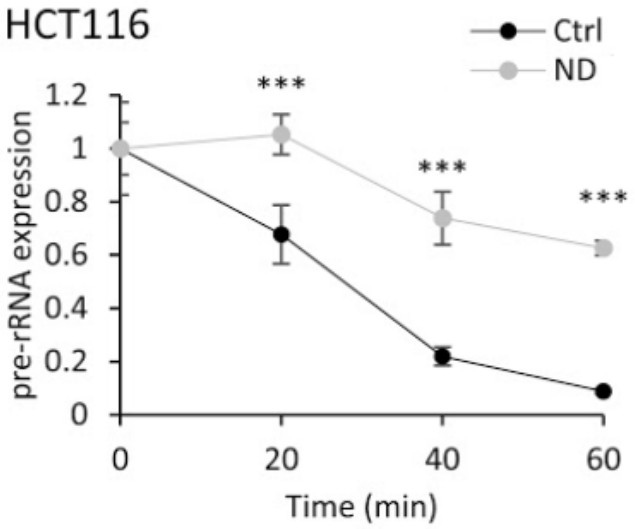

Figure 2.4: ND slows the turnover of pre-rRNAs, as assessed using qRT-PCR. HCT116 cells were pretreated to ND (24 h), transcription was stopped by Actinomycin D (40 μM) treatment, and total RNA was collected from cell lysates at the indicated time points. Half-life was approximated using linear regression. Control pre-rRNA half-life was 28 minutes while ND pre-rRNA half-life was greater than 60 minutes.

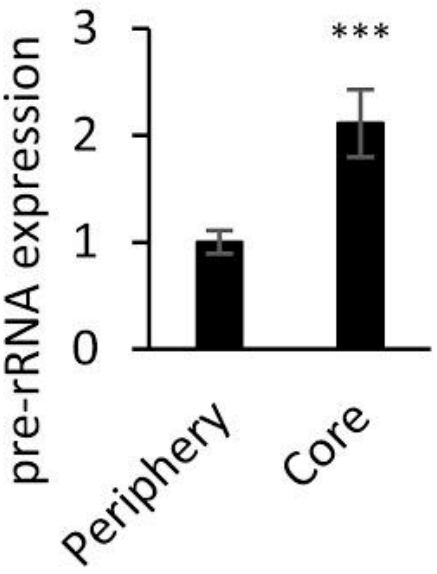

Figure 2.5: Pre-rRNA expression in the core and periphery of HCT116 tumors as assessed by qRT-PCR. Tumors were dissected into core and periphery regions (n = 8). Core pre-rRNA expression was normalized to periphery expression for each tumor.

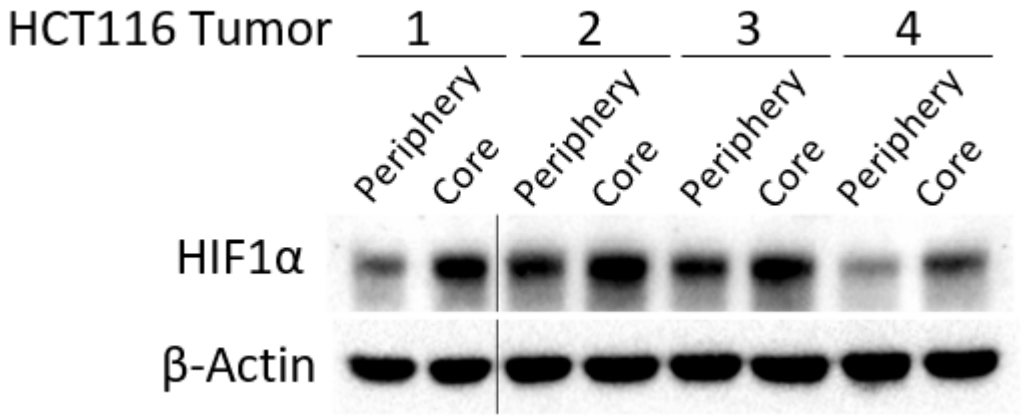

Figure 2.6: HIF1α expression in HCT116 periphery and core tumors.

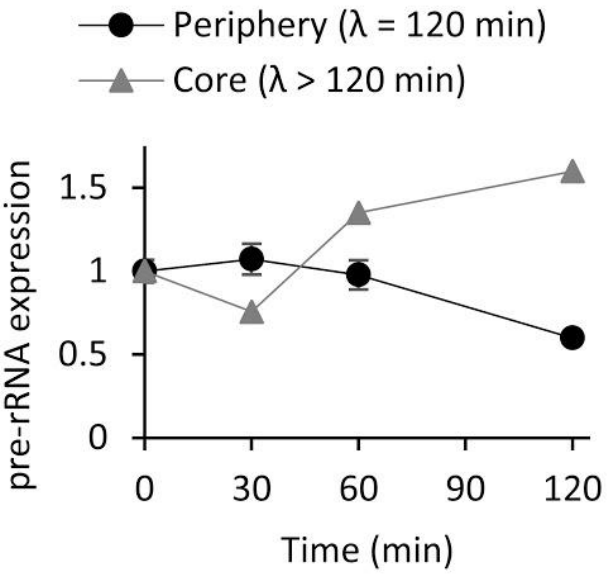

Figure 2.7: Pre-rRNA processing is faster in peripheral tissues compared to core tissues, as determined using qRT-PCR. Actinomycin D (1.67 mg/1000 mm3 tumor) was intratumorally injected into established HCT116 tumors and dissected into periphery and core samples at the indicated time points for RNA extraction. Each time point represents periphery and core tissues dissected from the same tumor.

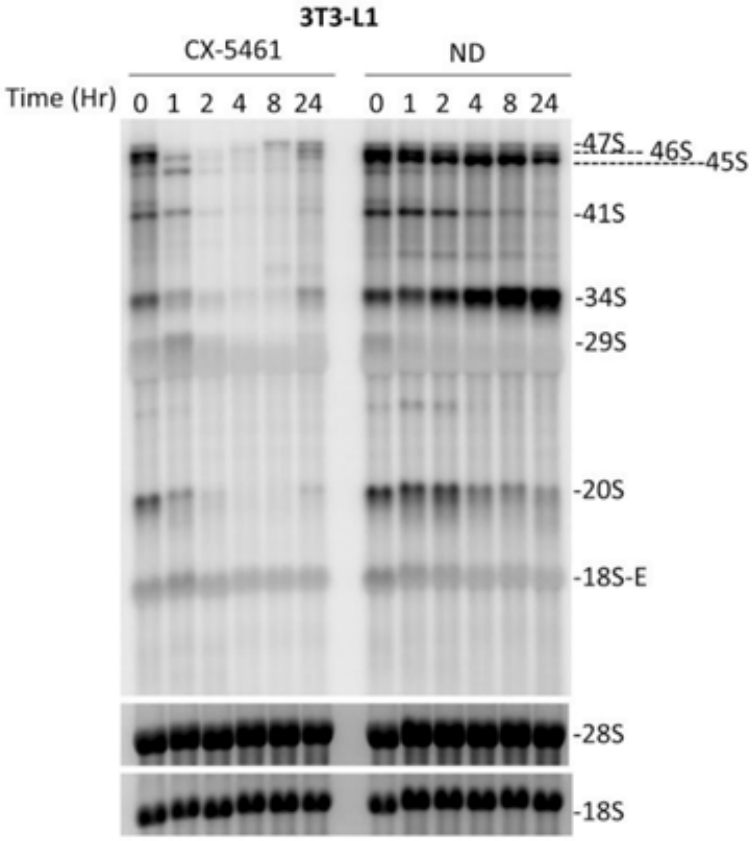

Figure 2.8: 3T3-L1 cells accumulate 34S pre-rRNA upon ND. 3T3-L1 cells were treated to control or ND at the indicated times and total RNA was collected from cell lysates and subjected to northern blot analysis (Probe: ITS-1)

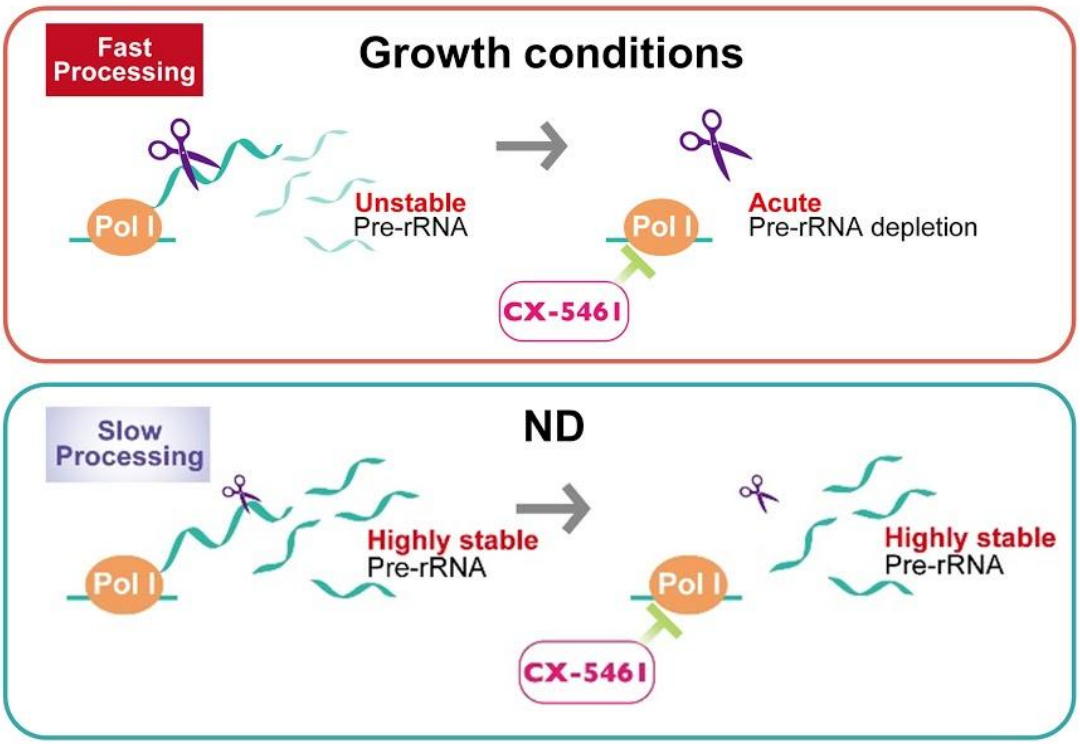

Figure 2.9: Top: Under growth conditions, when pre-rRNA processing is fast, CX-5461 acutely depletes the unstable pre-rRNAs. Bottom: Under ND, when pre-rRNA processing is slow, CX-5461 fails to acutely deplete stabilized pre-rRNAs.

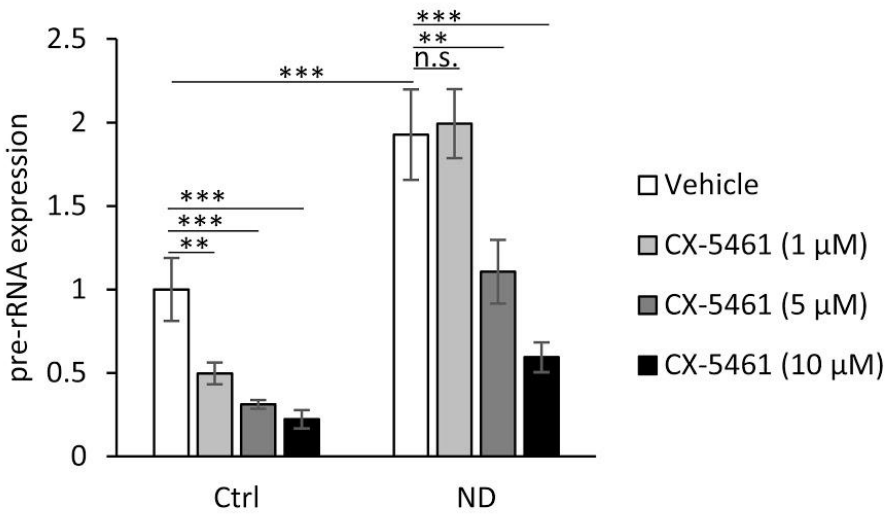

Figure 2.10: pre-rRNA expression (47S, 45S, 30S) in response to CX-5461 (8 h) under control or ND conditions, as determined using qRT-PCR. Cells were cultured to control or ND conditions in the presence of CX-5461 at the indicated concentrations for 8 h.

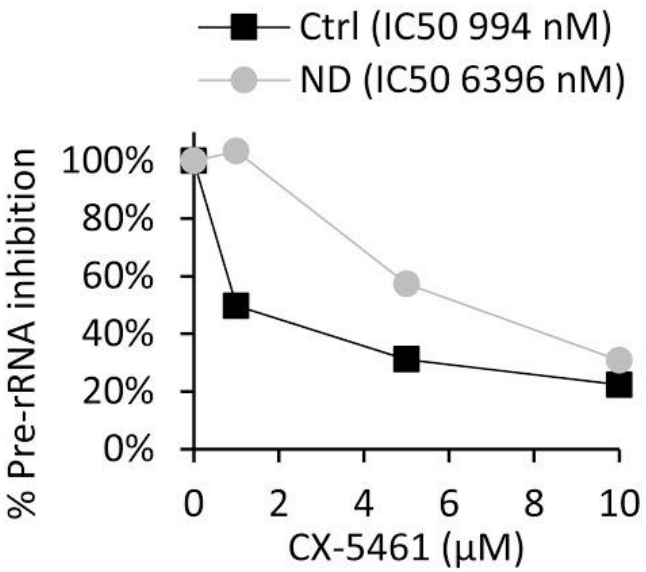

Figure 2.11: CX-5461 IC50 for %pre-rRNA inhibition compared to untreated control. Data from Figure 2.8 was normalized to the untreated control to calculate drug IC50.

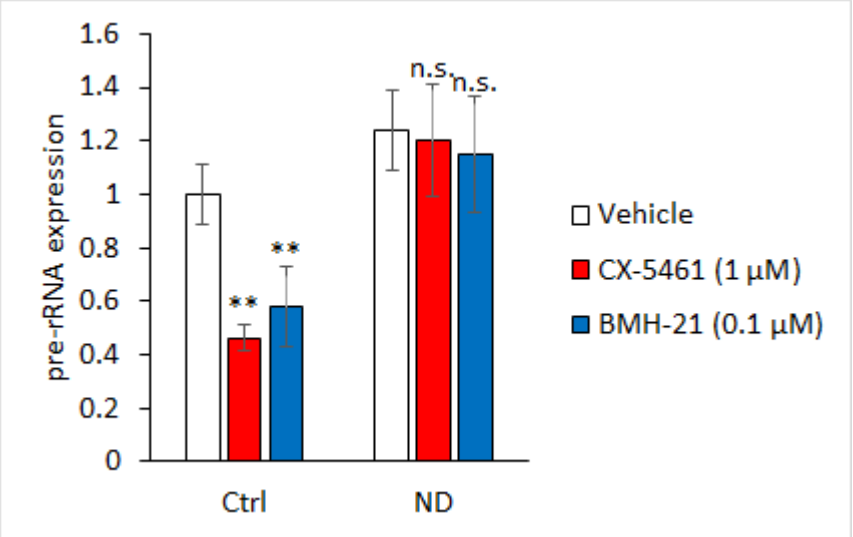

Figure 2.12: BMH-21 (0.1 uM) fails to inhibit pre-rRNA expression under ND.

Cells were cultured to control or ND conditions in the presence of CX-5461 or BMH-21 at the indicated concentrations for 8 h.

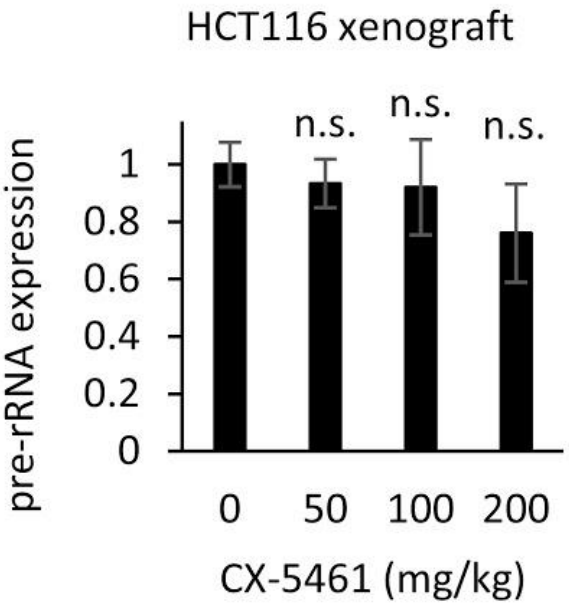

Figure 2.13: IP administration of up to 200 mg/kg CX-5461 failed to decrease pre-rRNA in HCT116 tumors, as determined using qRT-PCR. Mice were IP injected with vehicle (NaH2PO4) or CX-5461 at the indicated doses and tumors were harvested after 8 h for RNA isolation.

Chapter Three: HCT116 cells accumulate pre-rRNAs to resume ribosome biogenesis upon metabolic recovery without triggering the p53-dependent nucleolar stress response

Background and significance

The tumor suppressor protein p53 regulates a transcriptional program that induces cell cycle arrest or apoptosis(Vogelstein et al., 2000). Over half of human cancers display inactivating mutations in the *TP53* gene. *TP53* mutations in tumors start with loss by heterozygosity, followed by complete p53 deficiency(Bieging et al., 2014). p53 deficient tumors are typically more aggressive, characterized by genetic instability and increased metastatic potential. p53 activation is triggered by a variety of stresses, including DNA damage, replicative stress, hypoxia, and oxidative stress. Many of these stresses are commonly found *in vivo*. These stresses cause the E3 ubiquitin ligase MDM2 to dissociate from p53, thus allowing the accumulation of p53. Further, in addition to inactivating mutations in the *TP53* gene, cancer cells evolve secondary mechanisms to suppress the function of wild-type p53(Carrà et al., 2016). p53 mono-ubiquitination by Msl2 promotes cytoplasmic trapping of the tumor suppressor, thereby inhibiting the accumulation of p53 in the nucleus(Carrà et al., 2016; Kruse and Gu, 2009). Mdmx inhibits p53 by interfering with the transcriptional domain of p5 (Wade et al., 2013). MDM2 overexpression by amplification or promoter polymorphism restricts p53 function in many cancers by accelerating the degradation of p53(Oliner et al., 2016). In addition, many small molecule inhibitors of MDM2 have been developed to activate p53 in tumors(Shangary and Wang, 2009). Several of these MDM2 inhibitors, such as RG7112 and AMG 232, have been

advanced to human clinical trials to treat various cancers(Khurana and Shafer, 2019). However, MDM2 inhibitors can only suppress disease progression in tumors that harbor wildtype p53. In response to this problem, studies have demonstrated the feasibility of reactivating mutant p53 with small molecules such as PRIMA-1(Lewis, 2015).

I have shown that HCT116 cells accumulate pre-rRNAs under ND by slowing the kinetics of pre-rRNA processing according to nutrient availability. These findings were recapitulated *in vivo*, where pathophysiologic ND commonly found in tumors inhibited the pre-rRNA processing speed of tumor cells. As a consequence of slowed ND, tumor cells possessed highly stable pre-rRNAs that were resistant against Pol I inhibition by CX-5461. Interestingly, previous reports studying CX-5461 and its sister molecule CX-3543 only showed *in vitro* pre-rRNA depletion, but on-target drug activity *in vivo* was not reported. Given these data, we next sought to understand the biological role of pre-rRNAs under ND. It is unlikely that the pre-rRNA pool plays a role in the adaptation of cancer cells to severe nutrient depletion, because pre-rRNA synthesis itself is slowed under ND. Therefore, we aimed to study the importance of pre-rRNA accumulation to nutrient recovery.

Methods

Cell lines and Reagents

HCT116, A375, A549, U2OS, and MKN45, cells were purchased from the American Type Culture Collection (Manassas, VA, USA). HCT116 p53+/+ and p53−/− isogenic human colon cancer cells were kindly provided by Bert Vogelstein (Johns Hopkins University). HCT116, A375, A549, and U2OS cells were grown in Dulbecco's modified Eagle's medium (DMEM) (Nacalai Tesque, Kyoto, Japan), supplemented with 10% fetal bovine serum (FBS) (Thermo Fisher Scientific). MKN45 cells were maintained in RPMI (Nacalai Tesque, Kyoto, Japan), supplemented with 10% FBS. Cells were maintained at 37C in a 5% CO2 atmosphere in a humidified incubator. Nutrient deprivation medium was prepared to contain inorganic salts, i.e., 0.2 g/l CaCl2 (anhydrous), 0.1 mg/l Fe(NO3)3/9H2O, 0.4 g/l KCl, 97.67 mg/l MgSO4 (anhyd.), 6.4 g/l NaCl, 3.7 g/l NaHCO3, 0.125 g/l NaH2PO4/H2O, and 15 mg/l Phenol Red, according to the composition of DMEM. The compounds used in this study were obtained from: CX-5461 (MedChemExpress), AMG 232 (MedChemExpress), BMH-21 (Selleck), Camptothecin (Fujifilm Wako), Rapamycin (Fujifilm Wako), Torin1 (Fujifilm Wako), BEZ235 (Funakoshi), 5-Fluorouridine (TCI chemicals), Actinomycin D (Fujifilm Wako), zVAD-FMK (Fujifilm Wako),

Trypan Blue assays, MTT assays

For trypan blue exclusion assays, 6 x 10^5 cells (HCT116, A375, A549, U2OS) were seeded in 6-well plates and the percentage of cell death was determined after 24 h ND. Cell counting was performed with the TC20 Automated Cell Counter (Bio-Rad) according to the instructions of the manufacturer. After 24 h ND, the treatment

medium was set aside, adherent cells were detached with 100 µL trypsin/EDTA, and suspended with 900 µL of the treatment media. 100 µL of the suspension was mixed with 100 µL trypan blue solution (Bio-Rad) and analyzed with the TC20 Cell Counter.

For MTT assays, 6-10 x 10^5 cancer cells were seeded in 6-well plates, and after treatment, the cell media was aspirated and replaced with medium containing MTT (0.5 mg/mL) (Fujifilm Wako) for 3 h and lysed with DMSO. Absorbance was measured at 570 nm with a plate reader.

Western Blotting

Cells were lysed with RIPA buffer containing a protease protease inhibitor (P8340 Sigma), phosphatase inhibitors (P0044 and P5726 Sigma) and PMSF 1 mM. Protein quantification was performed using BCA kit (Pierce). Cell lysates were applied to a 10% polyacrylamide gel and transferred to a nitrocellulose membrane (Thermo Fisher Scientific). The membrane was incubated with antibodies that target p53 (1:1000, Calbiochem), b-actin (1:1000, Sigma-Aldrich), phospho-S6K (T389) (1:1000, Cell signaling technology), S6K (1:1000, Cell signaling technology), phospho-S6 (S235/236) (1:1000, Cell signaling technology), HIF-1alpha (1:1000 Novus Biologicals), Cleaved PARP (1:1000, Cell signaling technology) Caspase 3 (1:1000, Cell signaling technology), Cleaved Caspase 3 (1:1000, Cell signaling technology), PUMA (1:1000, Cell signaling technology), RPL5 (1:1000, kindly provided by Dr. Siniša Volarević), or RPL11 (1:1000, kindly provided by Dr. Siniša Volarević), followed by incubation with horseradish peroxidase-conjugated secondary antibodies (1:5000, Sigma-Aldrich). Signals were detected using

enhanced chemiluminescence detection reagents (Thermo Fisher Scientific) and images were acquired using a luminescent image analyzer (LAS3000, Fuji-Film, Japan).

RNA Isolation and quantitative RT-PCR

Total RNA was extracted from cells using the Isogen reagent (Nippon Gene, Toyama, Japan), converted to cDNA by using the Prime Script reverse transcriptase (Takara, Shiga, Japan) as per the manufacturer's instructions, and used for quantitative real-time PCR amplification using SYBR Green (Takara). Target RNA expression was normalized to β2m mRNA.

The following primer sequences were used:

For pre-rRNA expression:

5′-CCGCGCTCTACCTTACCTACCT-3'(forward);

5′-GCATGGCTTAATCTTTGAGACAAG-3′(reverse).

For human β2m:

5′-AGATGAGTATGCCTGCCGTG-3′;

5′-CATCCAATCCAAATGCGGCA-3′.

Results

Pre-rRNA accumulation is an adaptation to metabolic recovery

We first tested if pre-rRNA accumulation is a survival adaptation to ND. To investigate this, we decreased pre-rRNAs in HCT116 cells under ND by treatment with CX-5461 or BMH-21, and measured cell death using the trypan blue exclusion assay. Treatment with CX-5461 (10 μM) or BMH-21 (1 μM) strongly reduced pre-rRNA expression under control and ND conditions (**Fig 3.1**). To note, CX-5461 induces DNA damage at high concentrations, however, BMH-21 does not induce significant DNA damage when treated at 1 μM (Xu et al., 2017). Severe ND caused approximately half of the cell population to die after 24 h, but, in contrary to our hypothesis, CX-5461 and BMH-21 treatment strongly reduced cell death to approximately 25% (**Fig 3.2**). Thus, we concluded that pre-rRNA accumulation is not an adaptive response to ND. Notably, at the concentration of drug used, CX-5461 (10 μM) and BMH-21 (1 μM) did not cause any cell death under growth conditions despite potently activating p53 (**Fig 3.2, 3.3**). Such an uncoupling between cell death and p53 activation is consistent with a previous report showing that solid tumor cell lines respond to Pol I inhibition by entering cell cycle arrest regardless of p53 status(Rebello et al., 2016). Interestingly, ND blocked the activation of p53 by CX-5461 and BMH-21, indicating that Pol I inhibitors do not stabilize p53 in metabolically stressed cells (**Fig 3.3**). These results show that rRNA synthesis inhibitors do not kill growth-phase or nutrient-starved cancer cells.

We next wondered if pre-rRNA accumulation is an adaptation to metabolic recovery. We predicted that ND cells with low pre-rRNA would fail to resume proliferation upon nutrient restoration (**NR**). To induce metabolic recovery, pre-rRNA

expression was first decreased in HCT116 and A375 cells under ND (**Fig 3.4**), and after 24 h, the ND treatment media was removed and the cells were allowed to recover in drug-free basal media for another 24 h. Drug washout and NR allowed the control cells to recover and proliferate, however, pre-rRNA-depleted cells that were pre-treated with CX-5461 or BMH-21 underwent profound cell death during metabolic recovery (**Fig 3.5**). Cell death was not due to incomplete removal of the drug, as cells resume pre-rRNA synthesis after CX-5461 treatment and drug washout(Negi and Brown, 2015). In conclusion, metabolically stressed cancer cells accumulate pre-rRNAs to prevent nutrient-induced cell death during metabolic recovery.

Nutrient restoration induces the p53 nucleolar stress response in pre-rRNA depleted cells

During ribosome biogenesis, r-proteins bind sequentially to pre-rRNAs, and disruptions in this process causes unassembled uL5 and uL18 to bind and inhibit MDM2, leading to p53 stabilization (Bursać et al., 2012; Donati et al., 2013; Nicolas et al., 2016; Sloan et al., 2013). Additionally, active protein synthesis of uL5 and uL18 is absolutely required for the accumulation of unassembled uL5/uL18 that are capable of binding to MDM2(Bursać et al., 2012; Fumagalli et al., 2009). We therefore hypothesized that NR induces cell death by activating p53, and that p53 activation is caused by newly synthesized uL5/uL18 binding and inhibiting MDM2. In line with this, NR robustly activated p53 in pre-rRNA-depleted HCT116 and A375 cells (**Fig 3.6**). Next, to assess the expression of unassembled uL5 and uL18, crude lysates were subjected to ultracentrifugation to separate mature ribosomes from

soluble r-proteins (Bursać et al., 2012). This showed that NR caused uL5 and uL18 to accumulate in the ribosome-free fraction (**Fig 3.7**). Importantly, nucleolar stress causes uL5 and uL18 to bind to the 5S rRNA to form a trimeric ribonucleoprotein complex, and this trimeric complex binds and inhibits MDM2 to activate p53 (Donati et al., 2013; Nicolas et al., 2016; Sloan et al., 2013). In order to investigate the role of this trimeric complex in NR-mediated p53 activation, we performed a dual siRNA knockdown experiment of uL5 and uL18. Dual siRNA knockdown of uL5 and uL18 completely suppressed p53 activation (**Fig 3.8**), demonstrating that uL5/uL18 are directly involved in the nutrient-induced activation of p53. Independently silencing uL5 or uL18 also strongly abrogated NR-mediated p53 activation (**Fig 3.9**). Finally, NR did not induce apoptosis in p53-null HCT116 cells, as shown by the absence of cleaved PARP and cleaved caspase-3 (**Fig 3.10**). These results show that lethal synthesis of uL5 and uL18 drives p53 activation and subsequent cell death in pre-rRNA depleted cells during metabolic recovery.

Discussion

Ribosome biogenesis is tightly coordinated to nutrient availability, and at the same time, defects in ribosome biogenesis lead to the activation of p53 through the nucleolar stress response pathway (Yang et al., 2018). Yet, it is unknown how cancer cells regulate ribosome biogenesis during fluxes in nutrient availability in order to escape the p53-dependent nucleolar surveillance pathway. Upon observing that cancer cells accumulate pre-rRNAs under ND, we first tested if the pre-rRNA pool plays a role in cell survival under ND. However, inhibiting rRNA synthesis with CX-5461 or BMH-21 did not sensitize cells to severe ND, despite robustly decreasing pre-rRNA expression under ND. Unexpectedly, CX-5461 and BMH-21 strongly decreased cell death caused by 24 h ND in HCT116 cells. Since we have found that cells maintain Pol I transcriptional activity under ND, we speculate that blocking Pol I activity under ND protects cells from energy-depletion induced cell death. Indeed, since rRNA synthesis is an energy consuming process, it is tempting to speculate that CX-5461 and BMH-21 can help preserve energy balance in HCT116 cells under ND. Further, we observed that CX-5461 and BMH-21 robustly activated p53 in control cells but not ND cells. This suggested that the p53-dependent nucleolar surveillance pathway is inhibited by ND through an unknown mechanism. However, we speculate that ND inhibits p53 by blocking the translation of uL5 and uL18, which has been previously shown to be important in activating the p53 nucleolar stress response (Bursać et al., 2012; Fumagalli et al., 2009).

Finally, this data shows that cancer cells accumulate pre-rRNAs under ND in order to resume ribosome biogenesis upon nutrient restoration. Failure to accumulate

pre-rRNAs leads to newly synthesized uL5 and uL18 binding and inhibiting MDM2 during metabolic recovery, leading to the stabilization of p53. Given the importance of pre-rRNAs to metabolic recovery, it is not surprising that cancer cells maintain basal Pol I activity under ND. Indeed, the synthesis of pre-rRNAs under ND serves to facilitate metabolic recovery rather than cell survival under ND.

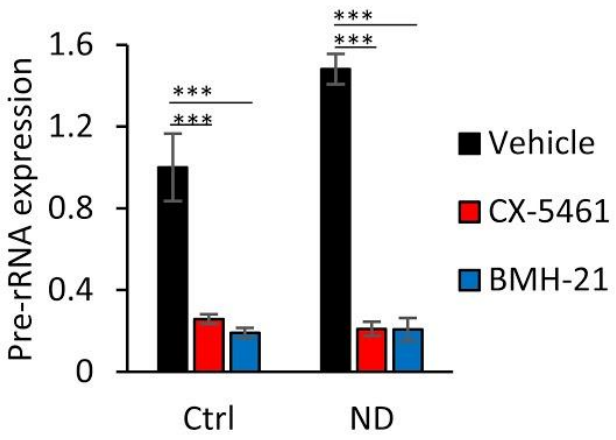

Figure 3.1: HCT116 pre-rRNA expression after treatment with vehicle (NaH2PO4), CX-5461 (10 μM), or BMH-21 (1 μM) under control or ND conditions (24 h). HCT116 cells were cultured to control or ND conditions in the presence of CX-5461 or BMH-21 for 24 h, and RNA was isolated for qRT-PCR analysis.

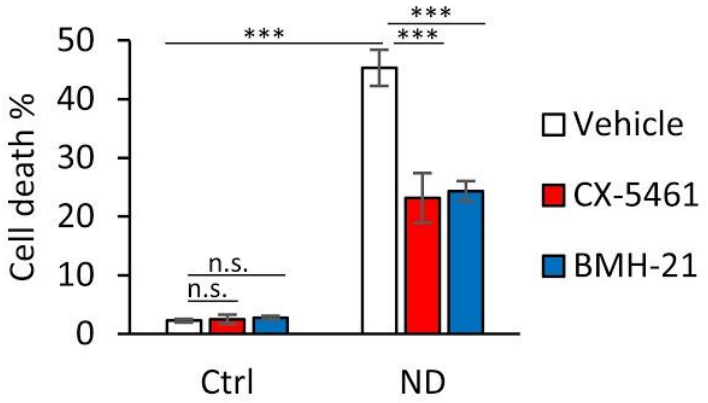

Figure 3.2: Percentage of cell death in HCT116 cells cultured in control or ND medium with vehicle (NaH2PO4), CX-5461 (10 μM), or BMH-21 (1 μM). HCT116 cells were cultured to control or ND conditions in the presence of CX-5461 or BMH-21 for 24 h, and cell death was assessed using the trypan blue exclusion assay (n=3).

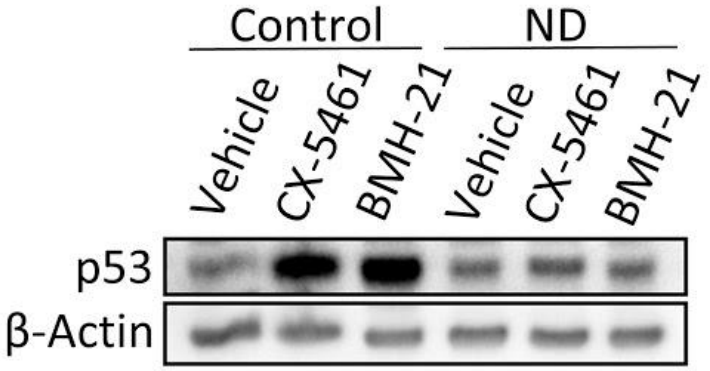

Figure 3.3: ND inhibited p53 activation by CX-5461 and BMH-21 as assessed using western blotting. HCT116 cells were cultured in control or ND medium with CX-5461 (10 μM) or BMH-21 (1 μM) for 8 h. HCT116 cells were cultured to control or ND conditions in the presence of CX-5461 or BMH-21 for 24 h, and protein was isolated for western blot analysis.

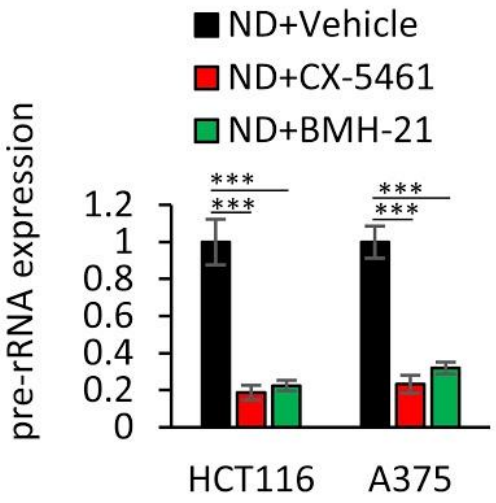

Figure 3.4: HCT116 and A375 pre-rRNA expression after treatment with vehicle (NaH2PO4), CX-5461 (10 μM), or BMH-21 (1 μM) under control or ND conditions (24 h). HCT116 and A375 cells were cultured to ND conditions in the presence of CX-5461 or BMH-21 for 24 h, and RNA was isolated for qRT-PCR analysis.

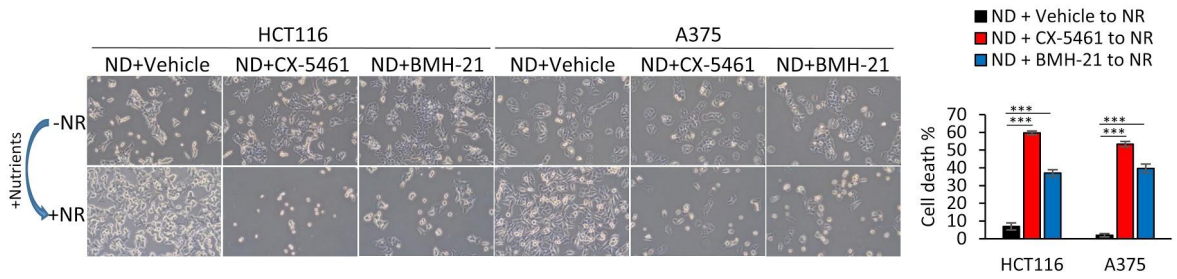

Figure 3.5: NR induces cell death in pre-rRNA depleted HCT116 and A375. Left: HCT116 and A375 cells under ND were treated with vehicle (NaH2PO4), CX-5461 (10 μM), or BMH-21 (1 μM) to inhibit pre-rRNA expression; after 24 h, the treatment medium was replaced with a drug-free basal medium (DMEM 10% FBS). Representative microscopy images were taken after 24 h of NR. Right: NR induces cell death in pre-rRNA depleted cells, as determined using trypan blue exclusion assay (n = 3).

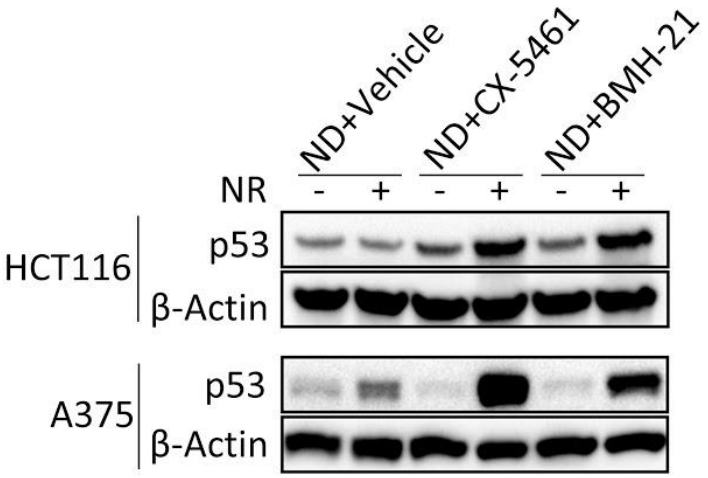

Figure 3.6: NR induces p53 in 'pre-rRNA depleted' HCT116 and A375 that were pre-treated to CX-5461/BMH-21 under ND, as assessed using western blotting. HCT116 and A375 cells were incubated under ND with vehicle (NaH2PO4), CX-5461 (10 μM), or BMH-21 (1 μM) for 24 h; after 24 h, the treatment medium was replaced with a drug-free basal medium for 8 h.

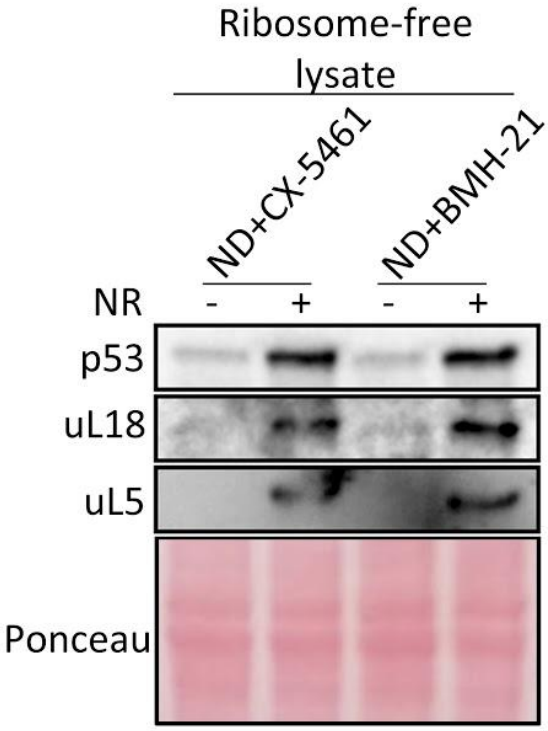

Figure 3.7: Expression of non-ribosomal uL5 and uL18 after NR. HCT116 were incubated under ND with vehicle (NaH2PO4) or CX-5461 (10 μM) for 24 h; after 24 h, the treatment medium was replaced with a drug-free basal medium for 8 h. After 8 h, the crude lysate was collected and subjected to ultracentrifugation to deplete the lysates of mature ribosomes. The ribosome-depleted lysate ("ribosome-free lysate") was then analyzed by western blotting to assess the expression of ribosome-free uL5 and uL18.

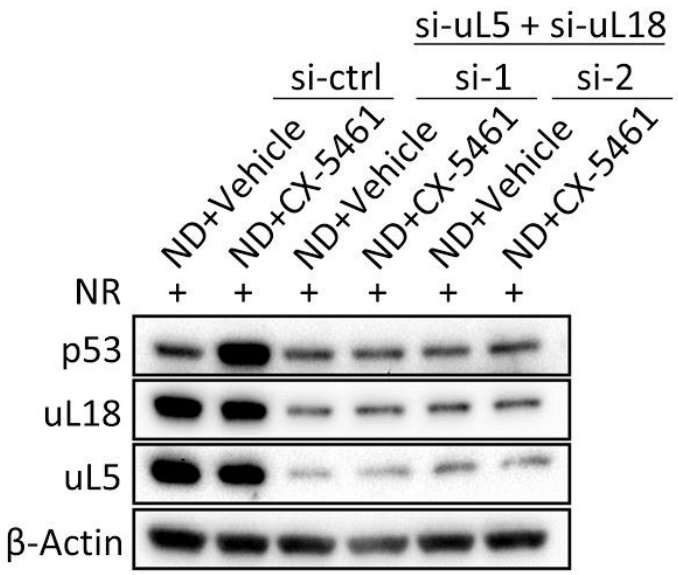

Figure 3.8: Co-knockdown of uL5 and uL18 by siRNA inhibits NR-mediated p53 activation. HCT116 cells were transfected with control or two different sets of siRNAs targeting uL5 and uL18. After 48 h, cells were placed under ND with CX-5461 (10 μM) for 24 h. After 24 h, the treatment medium was replaced with a drug-free basal medium for 8 h and the protein lysate was collected for western blotting.

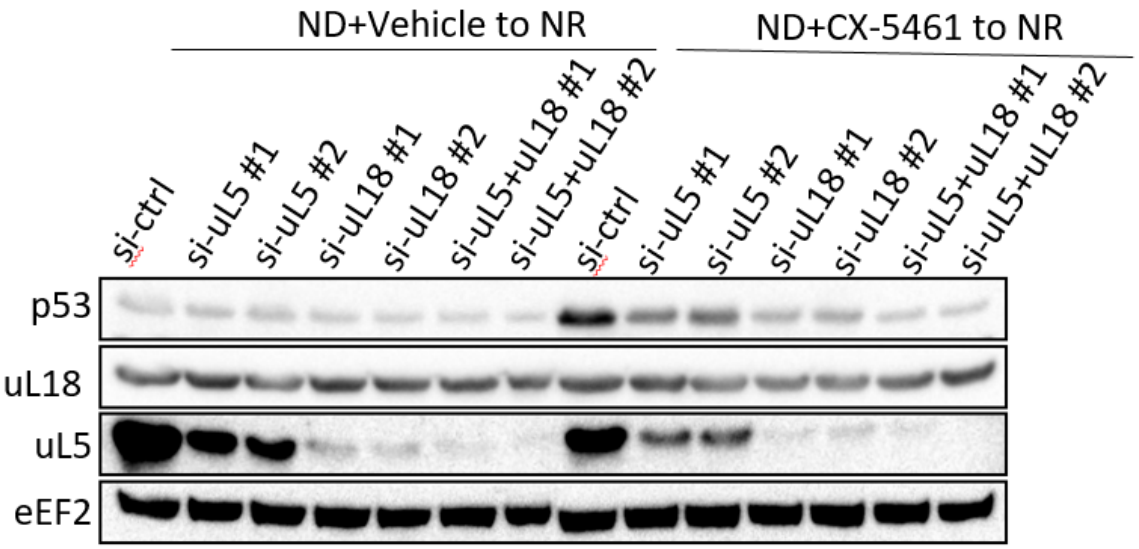

Figure 3.9: Independently silencing uL5 or uL18 decreases NR-mediated p53 activation. HCT116 cells were transfected with control or siRNAs targeting uL5 and uL18. After 48 h, cells were placed under ND with CX-5461 (10 μM) for 24 h. After 24 h, the treatment medium was replaced with a drug-free basal medium for 8 h and the protein lysate was collected for western blotting.

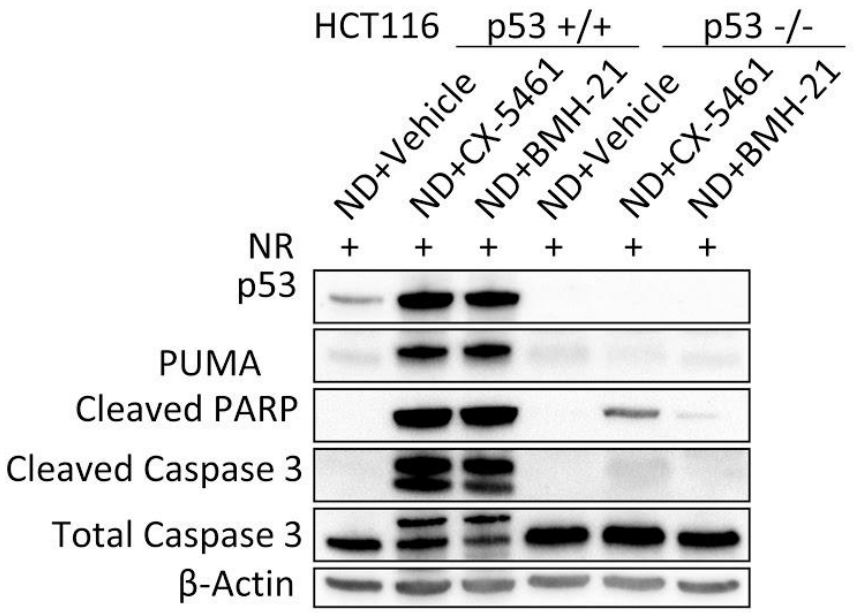

Figure 3.10: NR induces apoptosis in HCT116 p53 +/+ cells but not p53 -/- cells. HCT116 p53 +/+ or p53 -/- cells were incubated under ND with vehicle (NaH2PO4), CX-5461 (10 μM), or BMH-21 (1 μM) for 24 h; after 24 h, the treatment medium was replaced with a drug-free basal medium for 24 h and the protein lysate was collected for western blotting.

Chapter Four: Glutamine activates p53 via the Ras/Raf/MEK/ERK pathway

Background and Significance

Ribosome biogenesis requires the sophisticated assembly of 4 rRNAs and over 80 r-proteins(Lafontaine, 2015). Upon defects in ribosome biogenesis, accumulated uL5 and uL18 accumulate and bind to MDM2 in an inhibitory manner, leading to p53 stabilization(Donati et al., 2013; Nicolas et al., 2016; Sloan et al., 2013). However, it is important to highlight the fact that it is not ribosome-incorporated uL5 and uL18 that bind to MDM2, as ribosomal uL5/uL18 are already 'trapped' in the ribosome complexes and are thus unable to interact with MDM2. Rather, it is the newly translated population of uL5 and uL18 that is not yet incorporated into ribosomes that are capable of binding to MDM2. Like other nucleolar proteins, r-proteins are produced in the cytoplasm and are subsequently imported to the nucleus and nucleolus for ribosome assembly. Given this, it has been reported that *de novo* protein synthesis of uL5 and uL18 is absolutely critical for p53 stabilization by the nucleolar stress response(Bursać et al., 2012; Fumagalli et al., 2009). However, thus far, it is unknown what nutrients control the synthesis of uL5 and uL18, and what translational machinery regulates this production loop.

I have shown that cancer cells accumulate pre-rRNAs in order to resume ribosome biogenesis upon metabolic recovery without triggering the p53-dependent nucleolar surveillance pathway. Further, the ribosomal proteins uL5 and uL18 were responsible for driving p53 stabilization by NR. The stabilization of p53 through the nucleolar stress response requires the active translation of uL5 and uL18, indicating that

accumulation of p53 protein serves as a marker for continued uL5/uL18 synthesis. Thus, by assessing p53, we had a proxy measure for elucidating which nutrient(s) is responsible or required for inducing uL5 and uL18 synthesis.

Methods

Cell lines and Reagents

HCT116, A375, A549, U2OS, and MKN45, cells were purchased from the American Type Culture Collection (Manassas, VA, USA). HCT116 p53+/+ and p53−/− isogenic human colon cancer cells were kindly provided by Bert Vogelstein (Johns Hopkins University). HCT116, A375, A549, and U2OS cells were grown in Dulbecco's modified Eagle's medium (DMEM) (Nacalai Tesque, Kyoto, Japan), supplemented with 10% fetal bovine serum (FBS) (Thermo Fisher Scientific). MKN45 cells were maintained in RPMI (Nacalai Tesque, Kyoto, Japan), supplemented with 10% FBS. Cells were maintained at 37C in a 5% CO2 atmosphere in a humidified incubator. Nutrient deprivation medium was prepared to contain inorganic salts, i.e., 0.2 g/l CaCl2 (anhydrous), 0.1 mg/l Fe(NO3)3/9H2O, 0.4 g/l KCl, 97.67 mg/l MgSO4 (anhyd.), 6.4 g/l NaCl, 3.7 g/l NaHCO3, 0.125 g/l NaH2PO4/H2O, and 15 mg/l Phenol Red, according to the composition of DMEM. Glutamine deprivation was performed with DMEM without glutamine (Fujifilm Wako 045-30285) supplemented with 10% FBS. Glutamine replete medium was made by adding 4 mM L-glutamine (Fujifilm Wako) to the glutamine deprivation medium. Glucose deprivation was performed with DMEM without glucose (Fujifilm Wako 042-32255) supplemented with 10% FBS. Glucose replete medium was made by adding 25 mM D-glucose (Fujifilm Wako) to the glucose deprivation medium.

Tyrosine, leucine, and methionine medium were prepared according to the composition of DMEM (Nissui, Tokyo, Japan).

The compounds used in this study were obtained from: CX-5461 (MedChemExpress), AMG 232 (MedChemExpress), BMH-21 (Selleck), Camptothecin (Fujifilm Wako), Rapamycin (Fujifilm Wako), Torin1 (Fujifilm Wako), BEZ235 (Funakoshi), 5-Fluorouridine (TCI chemicals), Actinomycin D (Fujifilm Wako), zVAD-FMK (Fujifilm Wako),

Western Blotting

Cells were lysed with RIPA buffer containing a protease protease inhibitor (P8340 Sigma), phosphatase inhibitors (P0044 and P5726 Sigma) and PMSF 1 mM. Protein quantification was performed using BCA kit (Pierce). Cell lysates were applied to a 10% polyacrylamide gel and transferred to a nitrocellulose membrane (Thermo Fisher Scientific). The membrane was incubated with antibodies that target p53 (1:1000, Calbiochem), b-actin (1:1000, Sigma-Aldrich), phospho-S6K (T389) (1:1000, Cell signaling technology), S6K (1:1000, Cell signaling technology), phospho-S6 (S235/236) (1:1000, Cell signaling technology), HIF-1alpha (1:1000 Novus Biologicals), Cleaved PARP (1:1000, Cell signaling technology)

Caspase 3 (1:1000, Cell signaling technology), Cleaved Caspase 3 (1:1000, Cell signaling technology), PUMA (1:1000, Cell signaling technology), RPL5 (1:1000, kindly provided by Dr. Siniša Volarević), or RPL11 (1:1000, kindly provided by Dr. Siniša Volarević), followed by incubation with horseradish peroxidase-conjugated secondary antibodies (1:5000, Sigma-Aldrich). Signals were detected using enhanced chemiluminescence detection reagents (Thermo Fisher Scientific) and

images were acquired using a luminescent image analyzer (LAS3000, Fuji-Film, Japan).

RNA Isolation and quantitative RT-PCR

Total RNA was extracted from cells using the Isogen reagent (Nippon Gene, Toyama, Japan), converted to cDNA by using the Prime Script reverse transcriptase (Takara, Shiga, Japan) as per the manufacturer's instructions, and used for quantitative real-time PCR amplification using SYBR Green (Takara). Target RNA expression was normalized to β2m mRNA. For polysome isolation, cellular extracts were ultracentrifuged on a 35% sucrose cushion at 149,000 g x 2 h.

The following primer sequences were used:

For pre-rRNA expression:

5′-CCGCGCTCTACCTTACCTACCT-3'(forward);

5′-GCATGGCTTAATCTTTGAGACAAG-3′(reverse).

For human β2m:

5′-AGATGAGTATGCCTGCCGTG-3′;

5′-CATCCAATCCAAATGCGGCA-3′.

Results

Restoring the non-essential amino acid glutamine alone was sufficient to rescue p53 in pre-rRNA depleted HCT116 and A375 cells (**Fig 4.1**). Glutamine also stimulated the phosphorylation of S6K (**Fig 4.1**), consistent with its role in activating mTORC1(Durán et al., 2012; Villar et al., 2017). These results imply that glutamine restoration stimulates mTORC1-mediated translation to induce uL5 and uL18 synthesis, leading to inhibition of MDM2 and activation of p53. Together, these results show that glutamine 'metabolically activates' p53 in cells depleted of pre-rRNA by inducing synthesis of uL5 and uL18.

The translation of mRNAs encoding r-proteins (including uL5 and uL18) is regulated by a 5' terminal oligopyrimidine tract (5'TOP) and is positively regulated by mTORC1(Avni et al., 1997; Gentilella and Thomas, 2012). This raised the possibility that glutamine-induced synthesis of uL5 and uL18 required mTORC1 signalling. To test this, pre-rRNA depleted cells were re-fed glutamine in the presence of rapamycin or Torin1, two highly potent and specific mTORC1 inhibitors. However, contrary to our hypothesis, rapamycin and Torin1 did not affect the metabolic accumulation of p53 (**Fig 4.2**). Since p53 is a marker for uL5 and uL18 translation(Bursać et al., 2012; Fumagalli et al., 2009), this result suggested to us that the suppression of mTORC1 leads to the attenuation— but not complete blockade — of uL5/uL18 synthesis. Indeed, we reasoned that if uL5 and uL18 were still being synthesized at lowered levels under mTORC1 suppression, this would account for how rapamycin and Torin1 failed to inhibit p53. Additionally, a previous study found that mTORC1 suppression does not inhibit activation of p53 by nucleolar stress(Devlin et al., 2016), reinforcing the notion that synthesis of uL5 and uL18 is

not solely dependent on mTORC1. Together, these results suggest that glutamine-mediated synthesis of uL5 and uL18 is dependent on another signalling pathway in addition to mTORC1.

We therefore asked whether other growth-related pathways, such as the Ras-driven Raf/MEK/ERK pathway, might be involved in uL5 and uL18 translation. Due to the lack of inhibitors for Ras(Stephen et al., 2014), we tested if two highly selective pan-Raf inhibitors— LY3009210 and AZ628— could affect p53 protein levels. Strikingly, both Raf inhibitors completely blocked p53 activation by glutamine (**Fig 4.3**). Moreover, glutamine strongly induced MEK phosphorylation (**Fig 4.3**), showing that glutamine stimulates the Ras/Raf/MEK/ERK cascade. Next, to show that Raf suppression inhibits the translation of uL5 and uL18, we measured the expression of translationally active polysome-bound uL5/uL18 mRNAs. Glutamine restoration increased the expression of polysome-bound uL5 and uL18 mRNAs, and LY3009210 and AZ628 strongly inhibited this effect (**Fig 4.4**). Together, these results indicate that glutamine translationally activates uL5 and uL18 through the Ras/Raf/MEK/ERK cascade.

We have indirect evidence suggesting that uL5 and uL18 translation is not solely dependent on mTORC1 (**Fig 4.2**). Further, mTORC1 primarily regulates translation initiation(Mamane et al., 2006). We therefore reasoned that Ras/Raf/MEK/ERK might regulate the translation of uL5 and uL18 via the elongation step of translation. Indeed, in unstressed cells, ERK signalling facilitates protein synthesis by inhibiting eEF2K, a key negative regulator of translation elongation (**Fig 4.5**)(2017; Wang et al., 2014). Upon inhibition of eEF2K mediated by the ERK/p90RSK pathway, the downstream eukaryotic elongation factor eEF2 remains in its active

unphosphorylated form and promotes global protein synthesis (**Fig 4.5**)(2017; Wang et al., 2014). eEF2 mediates the translocation stage of translation elongation, *i.e.*, movement of the nascent peptide from the A-site to the P-site of the ribosome and of the ribosome along the mRNA by one codon(2017; Wang et al., 2014). Thus, we hypothesized that Ras/Raf/MEK/ERK signalling promotes uL5 and uL18 synthesis by activating eEF2-mediated translation elongation (**Fig 4.5**). We therefore assayed levels of eEF2 phosphorylation, phosphorylated eEF2 (Thr56) being the inactivated form that leads to the arrest of general protein synthesis(2017; Wang et al., 2014). Indeed, Raf suppression massively increased the phosphorylation of eEF2 (**Fig 4.3**). This suggested that Raf suppression inhibits uL5 and uL18 synthesis by blocking general protein synthesis that is normally mediated by active, unphosphorylated eEF2. Unexpectedly, we found that LY3009210 and AZ628 also inhibited mTORC1, as shown by the decreased phosphorylation of S6, S6K, and 4E-BP1 (**Fig 4.3**). We concluded that glutamine activates mTORC1 through Raf. Together, these results indicate that glutamine-induced synthesis of uL5 and uL18 requires Raf-dependent eEF2-mediated translation elongation. Further, in addition to the known role of mTORC1 in promoting the translation of r-proteins(Avni et al., 1997; Gentilella and Thomas, 2012), we conclude that glutamine induces uL5 and uL18 synthesis by activating Raf-dependent mTORC1 signalling.

Discussion

Under amino acid deprivation, cancer cells inhibit mTORC1 to block mTORC1-mediated anabolic processes such as protein synthesis(Villar et al., 2017). Further, it has been shown that refeeding glutamine to amino acid-deprived cells reactivates mTORC1(Villar et al., 2017). Given this, we first hypothesized that refeeding glutamine to ND cells could also stimulate the synthesis of uL5 and uL18 by activating mTORC1. Indeed, when HCT116 cells were pre-treated to CX-5461 or BMH-21 under ND, refeeding glutamine to these cells robustly activated p53. Surprisingly, inhibiting mTORC1 with the highly specific inhibitors rapamycin and torin1 had no effect on the metabolic accumulation of p53. We reasoned that mTORC1 inhibition alone was not sufficient to completely block uL5 and uL18 synthesis, and thus could not affect the metabolic accumulation of p53. Notably, it has been shown that the Ras/Raf/MEK/ERK pathway controls rRNA synthesis by phosphorylating TIF-IA at Ser633 and Ser649(Zhao et al., 2003).

Since signalling pathways tend to regulate closely-related pathways (*i.e.* Pol I transcription and r-protein synthesis), we therefore hypothesized that Ras/Raf/MEK/ERK signalling also regulates the synthesis of r-proteins, including uL5 and uL18. Indeed, inhibiting Raf with two highly specific inhibitors completely blocked p53 activation by glutamine. Concomitantly, Raf suppression inactivated mTORC1 and eEF2, suggesting that Raf inhibition suppresses the translation of uL5 and uL18 by inactivating these translational machinery. Altogether, these data further show that the translation of uL5 and uL18 is dependent on Ras/Raf/MEK/ERK signalling, in which Ras/RAF/MEK/ERK stimulates mTORC1 and eEF2-mediated translation to promote the synthesis of uL5 and uL18.

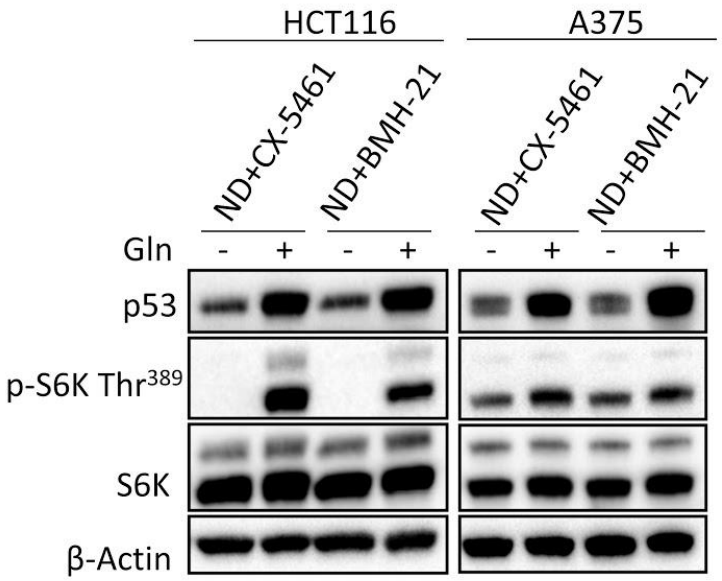

Figure 4.1: Glutamine (gln) activates p53 in pre-rRNA depleted HCT116 and A375 cells as assessed by western blotting. HCT116 and A375 cells were placed under ND with vehicle (NaH2PO4), CX-5461 (10 μM), or BMH-21 (1 μM) for 24 h. After 24 h the old treatment media was replaced with ND media containing PBS or Gln (4 mM) for 8 h.

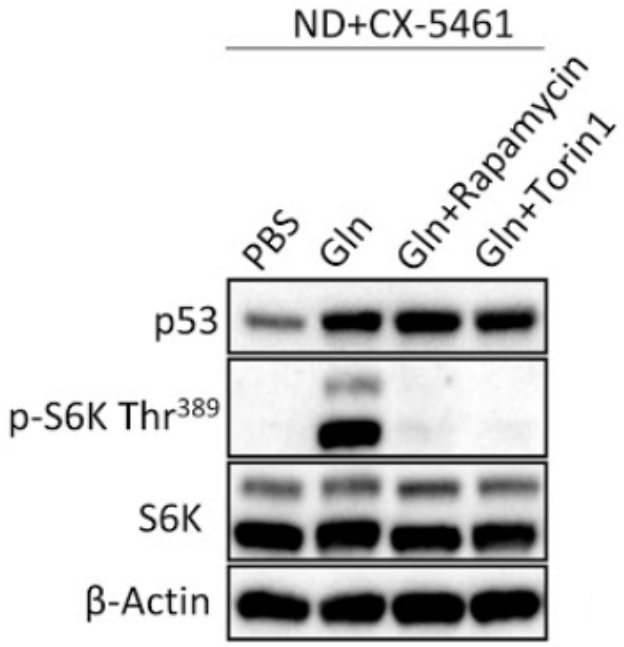

Figure 4.2: The effect of Rapamycin and Torin1 on p53 metabolic activation by glutamine (gln). HCT116 cells were placed under ND with CX-5461 (10 μM) for 24 h. After 24 h the old treatment media was replaced with ND media containing PBS, Gln (4 mM), or Gln (4mM) with Rapamycin/Torin1 (1 μM).

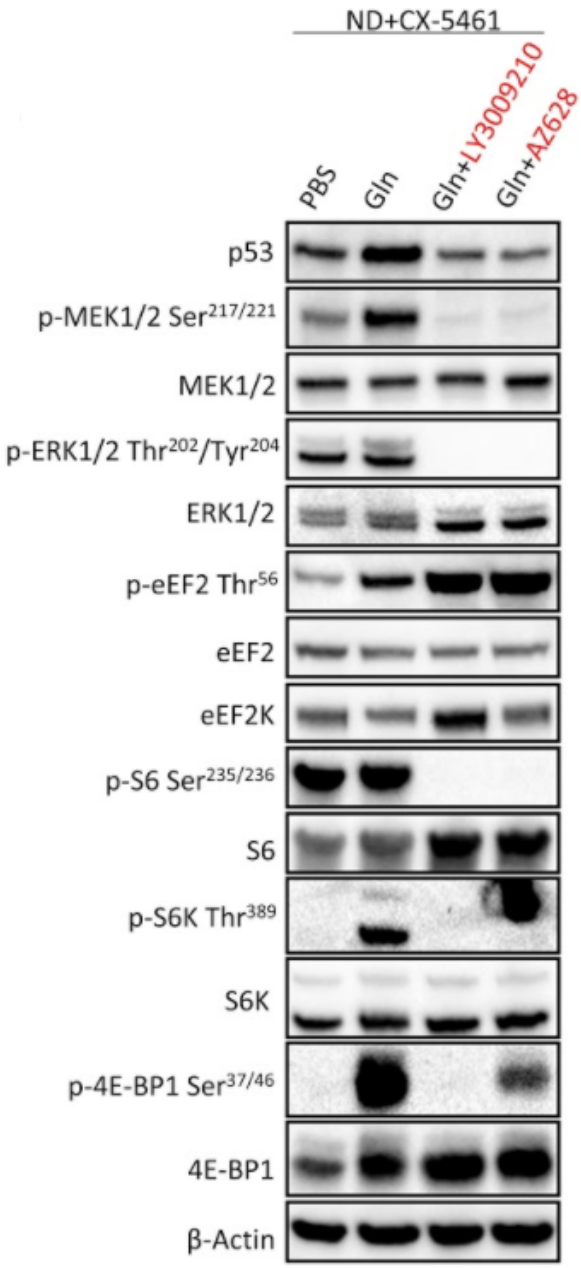

Figure 4.3: Inhibiting Raf with LY3009210 or AZ628 blocks p53 metabolic activation by glutamine (gln). HCT116 cells were placed under ND with CX-5461 (10 μM) for 24 h. After 24 h the old treatment media was replaced with ND media containing PBS, Gln (4 mM), or Gln (4mM) with LY3009210/AZ628 (1 μM).

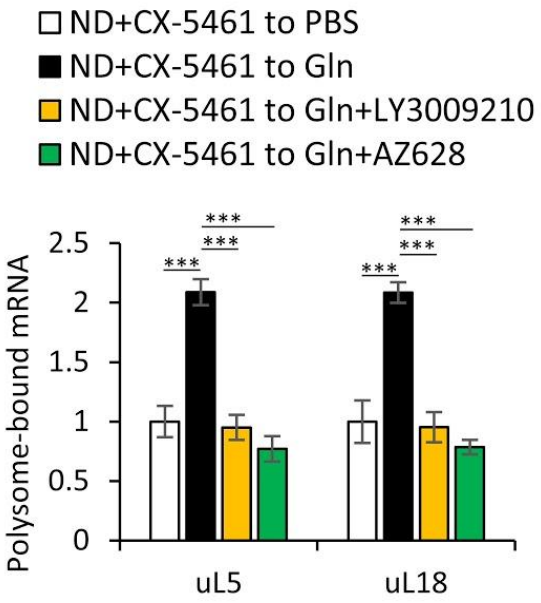

Figure 4.4: Expression of polysome-bound uL5 and uL18 mRNAs. HCT116 cells were placed under ND with CX-5461 (10 μM) for 24 h. After 24 h the old treatment media was replaced with ND media containing PBS, Gln (4 mM), or Gln (4mM) with LY3009210/AZ628 (1 μM). Polysomes were isolated via ultracentrifugation on a 35% sucrose cushion.

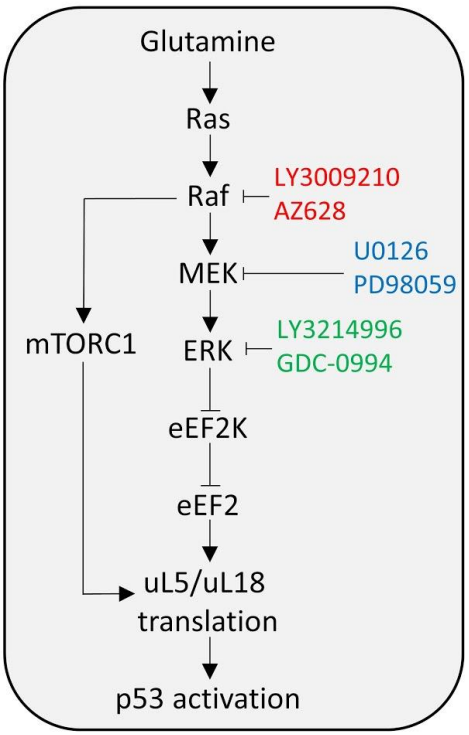

Figure 4.5: Schematic of the metabolic activation of p53 by glutamine: Restoring glutamine to ND cells activates Ras/Raf/MEK/ERK signaling, which inhibits eEF2K. Upon eEF2K inhibition, eEF2 remains in its active form to facilitate uL5/uL18 translation. Further, Raf activates mTORC1 to facilitate uL5/uL18 translation. Pharmacological inhibition of Raf leads to eEF2k activation, and upon eEF2k activation, eEF2 becomes inactivated and uL5/uL18 translation is blocked.

Chapter Five: Glutamine deprivation confers cancer cells resistance to RNA Pol I inhibitors by blocking the p53 nucleolar stress response

Background and Significance

Glutamine is a non-essential amino acid that becomes conditionally essential in rapidly proliferating cells (Hensley et al., 2013). Indeed, cancer cells display oncogene-dependent addictions to glutamine, and the withdrawal of glutamine can induce massive cell death in some cell lines (Hensley et al., 2013). In other cancer cell lines, glutamine withdrawal triggers growth arrest, but metabolic adaptations have been reported to occur, which allow cells to later grow in the chronic absence of glutamine(Hensley et al., 2013). The importance of glutamine is through its role as an anaplerotic substrate in the tricarboxylic acid (TCA) cycle, generating ATP and precursors for nucleotides and lipids (Altman et al., 2016). Upon being transported into the cell, glutamine is metabolized through 'glutaminolysis', which is the conversion of glutamine to alpha-ketoglutarate by glutamate dehydrogenase (GDH), glutamate pyruvate transaminase (GPT), and glutamate oxaloacetate (GOT)(Altman et al., 2016). Following this biochemical reaction, alpha-ketoglutarate is converted to succinyl-CoA and is subsequently consumed through the TCA cycle (Altman et al., 2016). Moreover, after glucose, glutamine is the second most highly consumed nutrient by cancer cell lines (Hosios et al., 2016; Jain et al., 2012). Given the importance of glutamine to cancer cell growth, it is not surprising that elevated glutamine consumption by tumor cells causes solid tumors to act as 'glutamine traps' (Klimberg et al., 1996). Given that the restoration of glutamine to pre-rRNA depleted cells can stabilize p53, we next tested the effect of glutamine deprivation on p53.

Methods

Cell lines, Reagents, and siRNA transfections

HCT116, A375, A549, U2OS, and MKN45, cells were purchased from the American Type Culture Collection (Manassas, VA, USA). HCT116 p53+/+ and p53−/− isogenic human colon cancer cells were kindly provided by Bert Vogelstein (Johns Hopkins University). HCT116, A375, A549, and U2OS cells were grown in Dulbecco's modified Eagle's medium (DMEM) (Nacalai Tesque, Kyoto, Japan), supplemented with 10% fetal bovine serum (FBS) (Thermo Fisher Scientific). MKN45 cells were maintained in RPMI (Nacalai Tesque, Kyoto, Japan), supplemented with 10% FBS. Cells were maintained at 37C in a 5% CO2 atmosphere in a humidified incubator. Nutrient deprivation medium was prepared to contain inorganic salts, i.e., 0.2 g/l CaCl2 (anhydrous), 0.1 mg/l Fe(NO3)3/9H2O, 0.4 g/l KCl, 97.67 mg/l MgSO4 (anhyd.), 6.4 g/l NaCl, 3.7 g/l NaHCO3, 0.125 g/l NaH2PO4/H2O, and 15 mg/l Phenol Red, according to the composition of DMEM. Glutamine deprivation was performed with DMEM without glutamine (Fujifilm Wako 045-30285) supplemented with 10% FBS. Glutamine replete medium was made by adding 4 mM L-glutamine (Fujifilm Wako) to the glutamine deprivation medium. Glucose deprivation was performed with DMEM without glucose (Fujifilm Wako 042-32255) supplemented with 10% FBS. Glucose replete medium was made by adding 25 mM D-glucose (Fujifilm Wako) to the glucose deprivation medium.

Tyrosine, leucine, and methionine medium were prepared according to the composition of DMEM (Nissui, Tokyo, Japan).

The compounds used in this study were obtained from: CX-5461 (MedChemExpress), AMG 232 (MedChemExpress), BMH-21 (Selleck),

Camptothecin (Fujifilm Wako), Rapamycin (Fujifilm Wako), Torin1 (Fujifilm Wako), BEZ235 (Funakoshi), 5-Fluorouridine (TCI chemicals), Actinomycin D (Fujifilm Wako), zVAD-FMK (Fujifilm Wako),

Cancer cells were transfected at ~30% confluency in 6-well plates with 5nM control or target siRNA using Lipofectamine RNAiMAX (Invitrogen) according to the instructions of the manufacturer. Control siRNA and siRNAs designed against p53, PUMA, RPL5, and RPL11 were obtained from Thermo Fisher Scientific.

Western Blotting

Cells were lysed with RIPA buffer containing a protease protease inhibitor (P8340 Sigma), phosphatase inhibitors (P0044 and P5726 Sigma) and PMSF 1 mM. Protein quantification was performed using BCA kit (Pierce). Cell lysates were applied to a 10% polyacrylamide gel and transferred to a nitrocellulose membrane (Thermo Fisher Scientific). The membrane was incubated with antibodies that target p53 (1:1000, Calbiochem), b-actin (1:1000, Sigma-Aldrich), phospho-S6K (T389) (1:1000, Cell signaling technology), S6K (1:1000, Cell signaling technology), phospho-S6 (S235/236) (1:1000, Cell signaling technology), HIF-1alpha (1:1000 Novus Biologicals), Cleaved PARP (1:1000, Cell signaling technology)

Caspase 3 (1:1000, Cell signaling technology), Cleaved Caspase 3 (1:1000, Cell signaling technology), PUMA (1:1000, Cell signaling technology), RPL5 (1:1000, kindly provided by Dr. Siniša Volarević), or RPL11 (1:1000, kindly provided by Dr. Siniša Volarević), followed by incubation with horseradish peroxidase-conjugated secondary antibodies (1:5000, Sigma-Aldrich). Signals were detected using enhanced chemiluminescence detection reagents (Thermo Fisher Scientific) and

images were acquired using a luminescent image analyzer (LAS3000, Fuji-Film, Japan).

RNA Isolation and quantitative RT-PCR

Total RNA was extracted from cells using the Isogen reagent (Nippon Gene, Toyama, Japan), converted to cDNA by using the Prime Script reverse transcriptase (Takara, Shiga, Japan) as per the manufacturer's instructions, and used for quantitative real-time PCR amplification using SYBR Green (Takara). Target RNA expression was normalized to β2m mRNA.

The following primer sequences were used:

For human p21:

5′-TGTCCGTCAGAACCCATGC-3′;

5′-AAAGTCGAAGTTCCATCGCTC-3′.

For human β2m:

5′-AGATGAGTATGCCTGCCGTG-3′;

5′-CATCCAATCCAAATGCGGCA-3′.

Cell line xenograft murine model:

All animal care procedures were in accordance with institutional guidelines approved by the University of Tokyo. HCT116 cells (5 × 106 in 100 μL PBS) were inoculated subcutaneously in the right flank of nude mice. Established tumors (~110–120 mm) were randomized into vehicle, CX-5461 (50mg/kg), or AMG 232 (50 mg/kg) treatment groups. Mice were treated with either oral gavage three times per week or

i.p. administration as indicated. Tumor volume was measured by external caliper, and tumor volume was calculated using the formula (l × w2)/2, where w = width and l = length in mm of the tumor. Mouse body weight was measured three times per week. After treatments, animals were euthanized, and tumors were harvested for further analysis

Results

Glutamine deprivation inhibits p53 activation by nucleolar stress

Thus far we have tested how adding back glutamine to starved pre-rRNA-depleted cells activates p53. We next sought to understand the effect of depriving cells of glutamine on the activation of p53 by the nucleolar surveillance pathway. To investigate this, we tested how glutamine deprivation affects the activation of p53 by CX-5461, which activates p53 via the uL5/uL18-dependent nucleolar surveillance pathway. Strikingly, glutamine deprivation blocked p53 activation by CX-5461, while the deprivation of glucose or other amino acids had no effect (**Fig 5.1**). Glutamine deprivation also inhibited p53 in A375, A549, U2OS, LNCaP, and MKN45 cells (**Fig 5.2**), consistent with hyper-elevated glutamine consumption being a hallmark of oncogenic transformation(Wise and Thompson, 2010). HCT116 cells under glutamine deprivation were highly resistant to CX-5461 (**Fig 5.3**), demonstrating that glutamine restriction confers resistance to rRNA synthesis inhibitors by blocking p53. Glucose deprivation, which does not inhibit p53, did not confer any resistance to CX-5461 (**Fig 5.3**). Finally, titration of extracellular glutamine showed suppression of p53 protein below 0.4 mM (**Fig 5.4**), which is approximately equal to the concentration of glutamine found in tumor xenografts (Pan et al., 2016). In conclusion, glutamine deprivation confers cancer cells resistance to CX-5461 by blocking the p53 nucleolar stress response.

Given that tumors are depleted of glutamine, we predicted that CX-5461 would display limited antitumor activity against solid tumors due to the inability to stabilize p53 *in vivo*. We selected HCT116 as our model cell line, since CX-5461 has been shown to potently inhibit HCT116 *in vitro* cell proliferation at an IC50 167 nM (Drygin

et al., 2011; Peltonen et al., 2014). Indeed, oral gavage of CX-5461 at the highest long-term tolerable dose (50 mg/kg) failed to significantly inhibit tumor growth (**Fig 5.5**). We used AMG 232, a non-genotoxic MDM2 inhibitor, as a positive control for p53-mediated tumor suppression. Oral gavage of AMG 232 (50 mg/kg) at the same dose and schedule as CX-5461 strongly suppressed HCT116 tumor growth (**Fig 5.5**). Further, IP injection of CX-5461 up to 200 mg/kg to HCT116 tumors failed to activate p53 while AMG 232 robustly induced p53 when treated at 50 mg/kg (**Fig 5.6**). These results indicate that tumoral glutamine deficiency hampers the antitumor activity of Pol I inhibitors by blocking the p53 nucleolar stress response.

Discussion

CX-5461 is a first-in-class RNA Pol I inhibitor that potently inhibits pre-rRNA synthesis and activates the p53-dependent nucleolar surveillance pathway (Pelletier et al., 2018). Various publications have shown that CX-5461 is highly effective at targeting p53 wildtype hematological malignancies (Bywater et al., 2012; Devlin et al., 2016; Hein et al., 2017), however, to date, it has not been shown that CX-5461 can activate p53 in solid tumors. Indeed, previous reports studying CX-5461 and BMH-21 showed that these molecules can activate p53 *in vitro*, but *in vivo* data was surprisingly missing (Drygin et al., 2011).

It has been shown that solid tumors are strongly depleted of glutamine due to elevated consumption by tumor cells (Pan et al., 2016). Since rapidly proliferating cells require glutamine, the addiction to glutamine is strongly associated with oncogenic transformation (Hensley et al., 2013). Thus, it is generally accepted that solid tumors in general are depleted of glutamine. Supporting this, Satoh *et al*. recently showed that colorectal adenocarcinomas were depleted of glutamine (along with glucose) when compared to other amino acids (Satoh et al., 2017). Given the physiological importance of glutamine deprivation to cancer biology, it would be interesting to perform a drug screen of common cancer therapeutics to understand the effect of glutamine deprivation on the therapeutic response.

We found that glutamine deprivation inhibits the activation of p53 by CX-5461, and these findings were reported in other solid tumor cell lines (A375, A549, U2OS, MKN45 cells). Since all tumor cell lines are addicted to glutamine, it is not surprising that this result was found in multiple cell lines in addition to HCT116 cells. Further, we showed that the deprivation of glucose, tyrosine, leucine, and methionine did not

affect the activation of p53 by CX-5461. These results explain why CX-5461 does not activate p53 in solid tumors and further suggests why p53 wild type solid tumors do not display sensitivity to CX-5461.

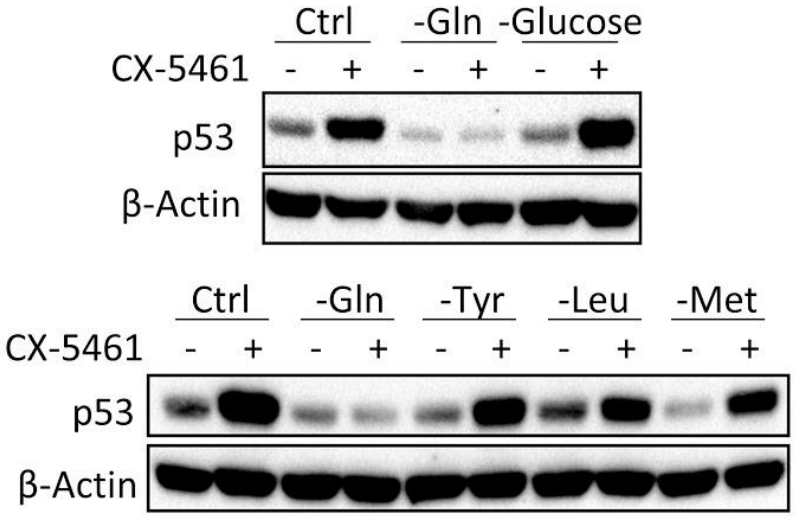

Figure 5.1: Deprivation of glutamine but not glucose, tyrosine, leucine, or methionine inhibited p53 activation by CX-5461. HCT116 cells were cultured in the respective starvation medium for 16 h followed by CX-5461 (1 μM) for 8 h.

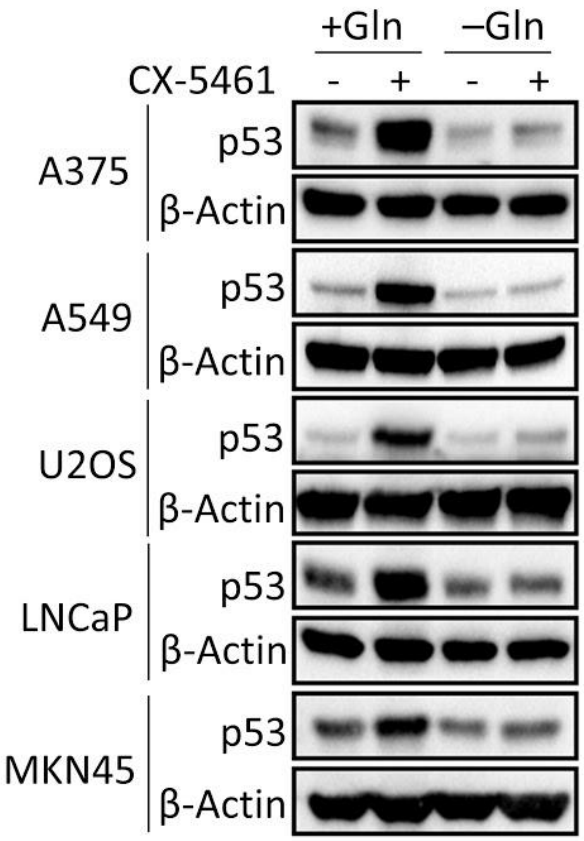

Figure 5.2: Glutamine deprivation inhibits p53 activation by CX-5461 (1 μM) in A375, A549, U2OS, LNCaP, and MKN45 cells. Cells were cultured in the respective starvation medium for 16 h followed by CX-5461 (1 μM) for 8 h.

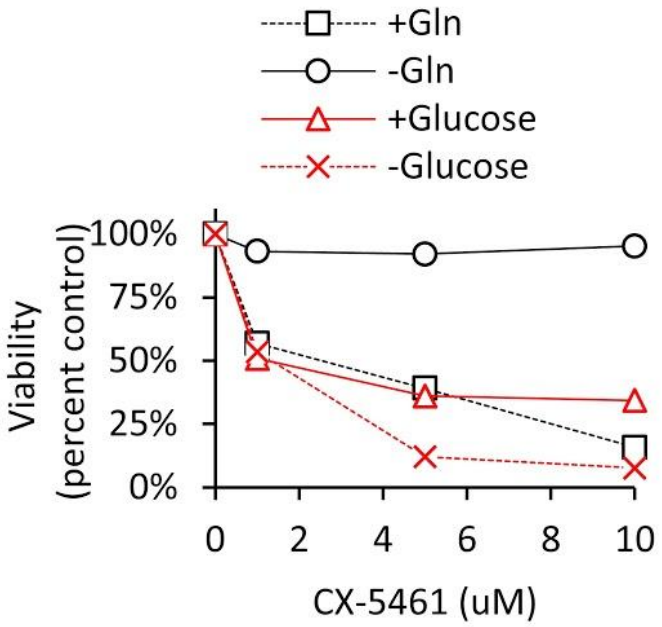

Figure 5.3: Deprivation of glutamine but not glucose conferred resistance to CX-5461 as assessed using MTT assay. HCT116 cells were incubated in the respective control or starvation medium with vehicle (NaH2PO4) or CX-5461 at the indicated concentrations for 72 h. Data points of each treatment was normalized to the respective vehicle-treated metabolic control.

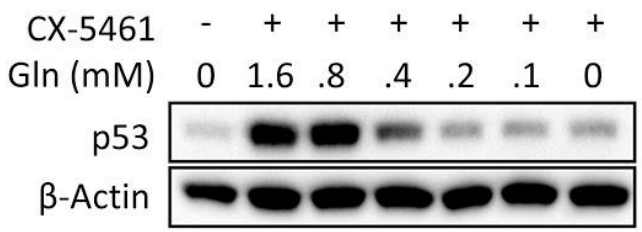

Figure 5.4: p53 activation by CX-5461 was suppressed under 0.4 mM glutamine as assessed by western blotting. HCT116 cells were cultured in the respective starvation medium for 16 h followed by CX-5461 (1 μM) for 8 h.

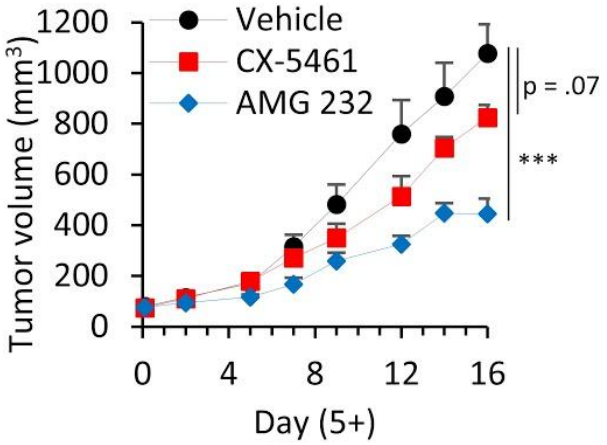

Figure 5.5: CX-5461 failed to inhibit HCT116 tumor growth. Mice were orally dosed with vehicle (NaH2PO4), CX-5461 (50 mg/kg), or AMG 232 (50 mg/kg) once daily three times per week. Drug treatment started 5 days post-implantation on tumors of approximately 75 mm3. Each point is the mean tumor volume ± stdev (n = 8/group).

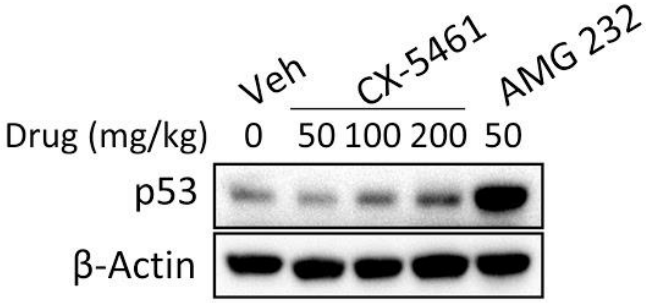

Figure 5.6: CX-5461 does not acutely stabilize p53 in HCT116 tumors. Mice were IP injected with vehicle (NaH2PO4), CX-5461 (50, 100, 200 mg/kg), or AMG 232 (50 mg/kg) and tumors were harvested after 8 h for western blot analysis.

Chapter Six: Discussion

Unstable vasculature in solid tumors leads to the development of tissue microenvironments that fluctuate in nutrient availability (Jones and Thompson, 2009). Tumor cells residing in such environments adapt to nutrient depletion by suppressing ATP-costly processes such as protein synthesis, nucleic acid synthesis, and ribosome biogenesis (Silvera et al., 2010), but how cells undertake metabolic recovery upon nutrient restoration remains unstudied. Here, we report that mammalian cells accumulate pre-rRNAs under starvation to escape nucleolar surveillance during metabolic recovery. We first observed that human cancer cells (colorectal HCT116, lung adenocarcinoma A549, osteosarcoma U2OS, gastric MKN45 cells) and mouse fibroblasts (3T3-L1 cells) modulate the kinetics of pre-rRNA processing according to nutrient availability in order to accumulate pre-rRNAs under nutrient deprivation. HCT116 cells accumulate pre-rRNAs by slowing pre-rRNA processing under ND. When nutrient stress resolves, recovering cells resume ribosome biogenesis and accumulated pre-rRNAs are bound by newly translated uL5 and uL18 for ribosomal subunit assembly. By rapidly associating with nascent uL5 and uL18, accumulated pre-rRNAs prevent uL5/uL18 from binding to MDM2, thereby enabling cellular escape from nucleolar surveillance during metabolic recovery. Conversely, using CX-5461 or BMH-21 to inhibit pre-rRNA expression under nutrient deprivation results in uL5/uL18-mediated p53 stabilization upon nutrient restoration, leading to nutrient-induced apoptosis. Thus, we propose that cancer cells accumulate pre-rRNAs under ND in order to resume ribosome biogenesis upon nutrient restoration without triggering the p53-dependent nucleolar surveillance pathway. Our data shows that pre-rRNA accumulation during nutrient

deprivation is a stress adaptation that restrains the MDM2-binding activity of uL5 and uL18 during periods of metabolic recovery in the solid tumor microenvironment. The cellular need for a pre-rRNA pool also implies that protein synthesis resumes more quickly than pre-rRNA biosynthesis. This concept can be readily accepted considering that successful synthesis of pre-rRNA includes both transcription and processing, in which the latter process can take up to an hour. In parallel, it is generally known that protein synthesis requires several minutes depending on the size of the peptide. Thus, pre-rRNA accumulation is an adaptation that takes into account the time difference between uL5 and uL18 protein synthesis and pre-rRNA production and maturation.

Based on our finding that the kinetics of pre-rRNA processing is dependent on nutrient availability, we found that core cells in solid tumors display slower pre-rRNA processing speeds than periphery cells. This finding is consistent with a previous report showing that the core of tumors are severely deprived of nutrients when compared to the periphery of tumors (Pan et al., 2016). Thus, HCT116 solid tumors are composed of cells that possess slow and heterogeneous pre-rRNA processing kinetics. We further showed that slowed in vivo processing leads to highly stable pre-rRNAs that possess long half-lives, and consequently, treatment of CX-5461 to solid tumor bearing animals failed to acutely inhibit tumoral pre-rRNA expression. Notably, pioneering reports that studied the anticancer effects of Pol I inhibitors (CX-5461, CX-3543) did not present data demonstrating in vivo pre-rRNA depletion (Drygin et al., 2009, 2011). The lack of *in vivo* data in previous reports is consistent with our data, which shows that it is not possible for Pol I inhibitors to acutely deplete tumoral pre-rRNA. Our data explains why CX-5461 and other Pol I inhibitors fail to

demonstrate acute on-target activity in solid tumors. Notably, it should be highlighted that the rate of ribosome biogenesis can be inferred from the speed of pre-rRNA processing. For instance, under growth conditions, HCT116 cells possess pre-rRNAs with a half-life of approximately 28 minutes while under ND conditions, the pre-rRNAs possess a half-life of approximately 78 minutes because precursor processing is slowed. Thus, because ribosome biogenesis is slowed under ND, the pre-rRNA half-life is extended. This can be inferred to *in vivo* conditions, where the tumoral pre-rRNA half-life of HCT116 tumors was found to be 142 minutes, suggesting that *in vivo* cells produce ribosomes at a significantly slower rate than *in vitro* cells. This is consistent with the fact that cells within solid tumors experience stresses such as hypoxia, nutrient deprivation, pH acidity, and cell crowding. Since tumor cells *in vivo* produce ribosomes at a slower rate, this may reflect a second method of drug resistance against Pol I inhibitors such as CX-5461 and BMH-21, which directly target ribosome biogenesis. Indeed, if a critical process is occuring at a lower rate than previously thought, it is tempting to speculate that small molecules that target this critical process would display decreased effectiveness *in vivo*.

We identified glutamine as the key nutrient that metabolically activates p53 by inducing the synthesis of uL5 and uL18. We cultured cells in nutrient deprived media to block uL5 and uL18 translation, and by assessing p53 levels in cells depleted of pre-rRNA, we found that restoring glutamine alone rescued uL5/uL18 synthesis. The restoration of other amino acids (leucine, tyrosine, methionine) did not activate p53, showing that these amino acids do not play a role in the regulation of uL5 and uL18 translation. Thus, we present data showing that a lone nutrient (i.e. glutamine) can metabolically activate p53 by translationally activating uL5 and uL18. Surprisingly,

despite the known importance of mTORC1 in the translational control of 5'TOP mRNAs that encode r-proteins (including uL5 and uL18) (Thoreen et al., 2012), inhibition of mTORC1 with the potent inhibitors rapamycin or Torin1 treatment did not affect the stabilization of p53 by glutamine. Since the accumulation of p53 protein is a marker of uL5 and uL18 synthesis (Bursać et al., 2012), this observation suggested to us that uL5/uL18 translation was not solely dependent on mTORC1. This is consistent with a previous report showing that inactivating mTORC1 does not completely block protein synthesis but only moderately attenuates global protein synthesis (Thoreen et al., 2012). Rather, we found that pharmacologically inhibiting Raf/MEK/ERK completely blocked the accumulation of p53. Raf/MEK/ERK inhibition appeared to arrest the synthesis of uL5 and uL18 by inactivating eEF2 and mTORC1. Altogether, these results suggest that glutamine-induced synthesis of uL5 and uL18 is facilitated by Raf-dependent eEF2-mediated translation elongation in addition to Raf-dependent mTORC1-mediated translation initiation.

We found that glutamine deprivation confers resistance to CX-5461 by blocking the p53 nucleolar stress response. This finding was recapitulated in the low glutamine tumor microenvironment, where CX-5461 failed to stabilize p53 in HCT116 tumors and consequently showed little inhibitory effect on HCT116 tumor growth. In line with our findings, another study found that p53 wild-type HCT116 tumors are highly resistant to CX-5461 (Xu et al., 2017) despite being remarkably sensitive in vitro (Drygin et al., 2011). Thus, these results indicate that CX-5461 displays limited therapeutic benefit in vivo due to tumoral glutamine deficiency. Notably, previous work has shown that CX-5461 effectively inhibits A375 tumor growth31, yet, we did not find p53 accumulation in CX-5461-treated A375 tumors. Since CX-5461 can bind

to DNA G-quadruplex structures to induce DNA damage (Xu et al., 2017), we speculate that A375 cells are especially vulnerable to G-quadruplex stabilizers. Altogether, our data shows that tumoral glutamine deficiency hampers the effectiveness of Pol I inhibitors by blocking the p53 nucleolar stress response. These findings offer an explanation as to why the efficacy of CX-5461 is not associated with p53 wild-type status in solid tumor types. Further, these results explain why CX-5461 is highly effective against blood cancers (Bywater et al., 2012), in which severe pathological nutrient deprivation does not occur. Indeed, plasma glutamine concentrations are approximately 0.8 mM, which is twice higher than the concentration at which p53 is inhibited (= 0.4 mM glutamine). Further, since the rate of ribosome biogenesis is dependent on nutrient availability, this implies that cells of hematological malignancies possess higher rates of ribosome biogenesis than cells of solid tumors and are therefore more vulnerable to Pol I inhibitors.

In summary, our study unveils a stress adaptive program that suppresses p53 during fluctuations in nutrient availability in the solid tumor microenvironment. This adaptation was demonstrated in both human cancer cells and mouse fibroblasts. Accumulation of unprocessed rRNAs emerges as a critical survival mechanism that is exploited by starving tumor cells to complete metabolic recovery during nutrient stress resolution. Further, solid tumors that are inherently depleted of glutamine do not accumulate p53 in response to Pol I inhibitors, highlighting how the metabolic landscape of the tumor microenvironment can deeply influence the therapeutic response to nucleolar function disruptors.

In conclusion, we propose that accumulation of pre-rRNAs under ND allows cancer cells to resume ribosome biogenesis during NR without triggering the p53 nucleolar

stress response (**Fig 6.1**). Accumulated pre-rRNAs serve to titrate nascent uL5 and uL18 away from MDM2 during metabolic recovery, thereby allowing cells to escape nucleolar surveillance (**Fig 6.1**). Failure to accumulate pre-rRNAs during ND results in uL5/uL18-mediated activation of p53, leading to nutrient-induced p53-mediated apoptosis (**Fig 6.1**).

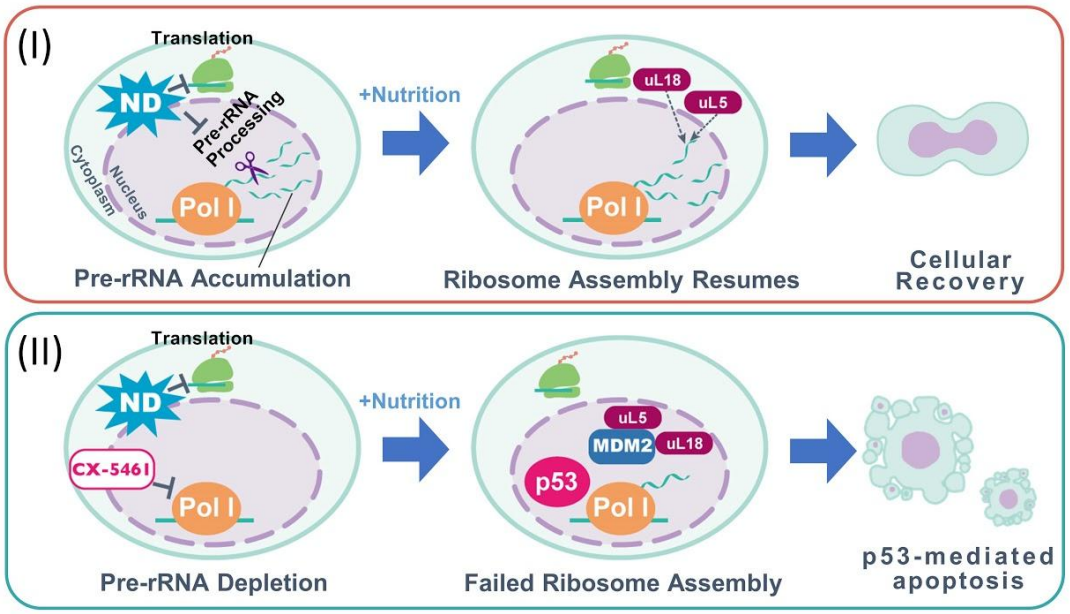

Figure 6.1: (Top: I) Cancer cells under ND accumulate pre-rRNA by severely slowing pre-rRNA processing. In parallel, ND suppresses global mRNA translation. Following nutrient addition (NR), accumulated pre-rRNAs are bound by newly translated uL5 and uL18 for ribosome assembly. (Bottom: II) Treatment with CX-5461 prevents cancer cells from accumulating pre-rRNAs under ND. Following NR, upon the absence of endogenous pre-rRNAs, nascent uL5 and uL18 binds to MDM2, leading to p53 stabilization and nutrient-induced apoptosis.

Acknowledgements

I thank the members of the Laboratory for Systems Biology and Medicine and Integrative Nutriomics and Oncology, RCAST, the University of Tokyo. I especially thank Dr. Osawa, Ms. Y. Nishida, Ms. R. Ando, Dr. T. Tanaka, Dr. H. Aburatani (RCAST, the University of Tokyo) for helpful discussions. I also thank Dr. Aburatani for providing the HCT116, A375, MKN45, and A549 cells. This work was supported by the MEXT scholarship program.

References

Ait Ouakrim, D., Pizot, C., Boniol, M., Malvezzi, M., Boniol, M., Negri, E., Bota, M., Jenkins, M.A., Bleiberg, H., and Autier, P. (2015). Trends in colorectal cancer mortality in Europe: retrospective analysis of the WHO mortality database. BMJ *351*, h4970.

Altman, B.J., Stine, Z.E., and Dang, C.V. (2016). From Krebs to clinic: glutamine metabolism to cancer therapy. Nat. Rev. Cancer *16*, 749.

Arnold, M., Sierra, M.S., Laversanne, M., Soerjomataram, I., Jemal, A., and Bray, F. (2017). Global patterns and trends in colorectal cancer incidence and mortality. Gut *66*, 683–691.

Arruebo, M., Vilaboa, N., Sáez-Gutierrez, B., Lambea, J., Tres, A., Valladares, M., and González-Fernández, A. (2011). Assessment of the evolution of cancer treatment therapies. Cancers *3*, 3279–3330.

Avni, D., Biberman, Y., and Meyuhas, O. (1997). The 5' Terminal Oligopyrimidine Tract Confers Translational Control on Top Mrnas in a Cell Type-and Sequence Context-Dependent Manner. Nucleic Acids Research *25*, 995–1001.

Banin, S. (1998). Enhanced Phosphorylation of p53 by ATM in Response to DNA Damage. Science *281*, 1674–1677.

Bertram, J.S. (2000). The molecular biology of cancer. Mol. Aspects Med. *21*, 167–223.

Bieging, K.T., Mello, S.S., and Attardi, L.D. (2014). Unravelling mechanisms of p53-mediated tumour suppression. Nature Reviews Cancer *14*, 359–370.

Bray, F., Ferlay, J., Soerjomataram, I., Siegel, R.L., Torre, L.A., and Jemal, A. (2018). Global cancer statistics 2018: GLOBOCAN estimates of incidence and mortality worldwide for 36 cancers in 185 countries. CA: A Cancer Journal for Clinicians *68*, 394–424.

Bursać, S., Brdovčak, M.C., Pfannkuchen, M., Orsolić, I., Golomb, L., Zhu, Y., Katz, C., Daftuar, L., Grabušić, K., Vukelić, I., et al. (2012). Mutual protection of ribosomal proteins L5 and L11 from degradation is essential for p53 activation upon ribosomal biogenesis stress. Proc. Natl. Acad. Sci. U. S. A. *109*, 20467–20472.

Buttgereit, F., and Brand, M.D. (1995). A hierarchy of ATP-consuming processes in mammalian cells. Biochemical Journal *312*, 163–167.

Bywater, M.J., Poortinga, G., Sanij, E., Hein, N., Peck, A., Cullinane, C., Wall, M., Cluse, L., Drygin, D., Anderes, K., et al. (2012). Inhibition of RNA polymerase I as a therapeutic strategy to promote cancer-specific activation of p53. Cancer Cell *22*, 51–65.

Carrà, G., Crivellaro, S., Taulli, R., Guerrasio, A., Saglio, G., and Morotti, A. (2016). Mechanisms of p53 Functional De-Regulation: Role of the IκB-α/p53 Complex. Int. J. Mol. Sci. *17*.

Chiarugi, V., Cinelli, M., Magnelli, L., and Dello Sbarba, P. Apoptosis: Molecular Regulation of Cell Death and Hematologic Malignancies. Hematologic Malignancies 323–338.

Clavell, L.A., Gelber, R.D., Cohen, H.J., Hitchcock-Bryan, S., Cassady, J.R., Tarbell, N.J., Blattner, S.R., Tantravahi, R., Leavitt, P., and Sallan, S.E. (1986). Four-agent induction and intensive asparaginase therapy for treatment of childhood acute lymphoblastic leukemia. N. Engl. J. Med. *315*, 657–663.

Costa-Mattioli, M., and Walter, P. (2020). The integrated stress response: From mechanism to disease. Science *368*.

Dekker, E., Tanis, P.J., Vleugels, J.L.A., Kasi, P.M., and Wallace, M.B. (2019). Colorectal cancer. Lancet *394*, 1467–1480.

Derenzini, M., Montanaro, L., and Treré, D. (2009). What the nucleolus says to a tumour pathologist. Histopathology *54*, 753–762.

Devlin, J.R., Hannan, K.M., Hein, N., Cullinane, C., Kusnadi, E., Ng, P.Y., George, A.J., Shortt, J., Bywater, M.J., Poortinga, G., et al. (2016). Combination Therapy Targeting Ribosome Biogenesis and mRNA Translation Synergistically Extends Survival in MYC-Driven Lymphoma. Cancer Discov. *6*, 59–70.

Dewhirst, M.W. (2018). A potential solution for eliminating hypoxia as a cause for radioresistance. Proc. Natl. Acad. Sci. U. S. A. *115*, 10548–10550.

Donati, G., Peddigari, S., Mercer, C.A., and Thomas, G. (2013). 5S ribosomal RNA is an essential component of a nascent ribosomal precursor complex that regulates the Hdm2-p53 checkpoint. Cell Rep. *4*, 87–98.

Drygin, D., Siddiqui-Jain, A., O'Brien, S., Schwaebe, M., Lin, A., Bliesath, J., Ho, C.B., Proffitt, C., Trent, K., Whitten, J.P., et al. (2009). Anticancer activity of CX-3543: a direct inhibitor of rRNA biogenesis. Cancer Res. *69*, 7653–7661.

Drygin, D., Lin, A., Bliesath, J., Ho, C.B., O'Brien, S.E., Proffitt, C., Omori, M., Haddach, M., Schwaebe, M.K., Siddiqui-Jain, A., et al. (2011). Targeting RNA polymerase I with an oral small molecule CX-5461 inhibits ribosomal RNA synthesis and solid tumor growth. Cancer Res. *71*, 1418–1430.

Durán, R.V., Oppliger, W., Robitaille, A.M., Heiserich, L., Skendaj, R., Gottlieb, E., and Hall, M.N. (2012). Glutaminolysis activates Rag-mTORC1 signaling. Mol. Cell *47*, 349–358.

Eagle, H. (1955). THE MINIMUM VITAMIN REQUIREMENTS OF THE L AND HELA CELLS IN TISSUE CULTURE, THE PRODUCTION OF SPECIFIC VITAMIN DEFICIENCIES, AND THEIR CURE. Journal of Experimental Medicine *102*, 595–600.

El-Naggar, A.M., Veinotte, C.J., Cheng, H., Grunewald, T.G.P., Negri, G.L., Somasekharan, S.P., Corkery, D.P., Tirode, F., Mathers, J., Khan, D., et al. (2015). Translational Activation of HIF1α by YB-1 Promotes Sarcoma Metastasis. Cancer Cell *27*, 682–697.

Fumagalli, S., Di Cara, A., Neb-Gulati, A., Natt, F., Schwemberger, S., Hall, J., Babcock, G.F., Bernardi, R., Pandolfi, P.P., and Thomas, G. (2009). Absence of nucleolar disruption after impairment of 40S ribosome biogenesis reveals an rpL11-translation-dependent mechanism of p53 induction. Nat. Cell Biol. *11*, 501–508.

Gentilella, A., and Thomas, G. (2012). The director's cut. Nature *485*, 50–51.

Goodman, L.S., and Wintrobe, M.M. (1946). Nitrogen mustard therapy; use of methyl-bis

(beta-chloroethyl) amine hydrochloride and tris (beta-chloroethyl) amine hydrochloride for Hodgkin's disease, lymphosarcoma, leukemia and certain allied and miscellaneous disorders. J. Am. Med. Assoc. *132*, 126–132.

Hanahan, D., and Weinberg, R.A. (2011). Hallmarks of cancer: the next generation. Cell *144*, 646–674.

Harris, A.L. (2002). Hypoxia--a key regulatory factor in tumour growth. Nat. Rev. Cancer *2*, 38–47.

Heidelberger, C., Chaudhuri, N.K., Danneberg, P., Mooren, D., Griesbach, L., Duschinsky, R., Schnitzer, R.J., Pleven, E., and Scheiner, J. (1957). Fluorinated pyrimidines, a new class of tumour-inhibitory compounds. Nature *179*, 663–666.

Hein, N., Cameron, D.P., Hannan, K.M., Nguyen, N.-Y.N., Fong, C.Y., Sornkom, J., Wall, M., Pavy, M., Cullinane, C., Diesch, J., et al. (2017). Inhibition of Pol I transcription treats murine and human AML by targeting the leukemia-initiating cell population. Blood *129*, 2882–2895.

Hensley, C.T., Wasti, A.T., and DeBerardinis, R.J. (2013). Glutamine and cancer: cell biology, physiology, and clinical opportunities. J. Clin. Invest. *123*, 3678–3684.

Holmberg Olausson, K., Nistér, M., and Lindström, M.S. (2012). p53 -Dependent and -Independent Nucleolar Stress Responses. Cells *1*, 774–798.

Hoppe, S., Bierhoff, H., Cado, I., Weber, A., Tiebe, M., Grummt, I., and Voit, R. (2009). AMP-activated protein kinase adapts rRNA synthesis to cellular energy supply. Proceedings of the National Academy of Sciences *106*, 17781–17786.

Hosios, A.M., Hecht, V.C., Danai, L.V., Johnson, M.O., Rathmell, J.C., Steinhauser, M.L., Manalis, S.R., and Vander Heiden, M.G. (2016). Amino Acids Rather than Glucose Account for the Majority of Cell Mass in Proliferating Mammalian Cells. Dev. Cell *36*, 540–549.

Ivan, M., Kondo, K., Yang, H., Kim, W., Valiando, J., Ohh, M., Salic, A., Asara, J.M., Lane, W.S., and Kaelin, W.G., Jr (2001). HIFalpha targeted for VHL-mediated destruction by proline hydroxylation: implications for O2 sensing. Science *292*, 464–468.

Jain, M., Nilsson, R., Sharma, S., Madhusudhan, N., Kitami, T., Souza, A.L., Kafri, R., Kirschner, M.W., Clish, C.B., and Mootha, V.K. (2012). Metabolite profiling identifies a key role for glycine in rapid cancer cell proliferation. Science *336*, 1040–1044.

Jones, R.G., and Thompson, C.B. (2009). Tumor suppressors and cell metabolism: a recipe for cancer growth. Genes Dev. *23*, 537–548.

Kamura, T., Conrad, M.N., Yan, Q., Conaway, R.C., and Conaway, J.W. (1999). The Rbx1 subunit of SCF and VHL E3 ubiquitin ligase activates Rub1 modification of cullins Cdc53 and Cul2. Genes Dev. *13*, 2928–2933.

Khot, A., Brajanovski, N., Cameron, D.P., Hein, N., Maclachlan, K.H., Sanij, E., Lim, J., Soong, J., Link, E., Blombery, P., et al. (2019). First-in-Human RNA Polymerase I Transcription Inhibitor CX-5461 in Patients with Advanced Hematologic Cancers: Results of a Phase I Dose-Escalation Study. Cancer Discov. *9*, 1036–1049.

Khurana, A., and Shafer, D.A. (2019). MDM2 antagonists as a novel treatment option for acute myeloid leukemia: perspectives on the therapeutic potential of idasanutlin (RG7388).

Onco. Targets. Ther. *12*, 2903–2910.

Kimura, H., Braun, R.D., Ong, E.T., Hsu, R., Secomb, T.W., Papahadjopoulos, D., Hong, K., and Dewhirst, M.W. (1996). Fluctuations in red cell flux in tumor microvessels can lead to transient hypoxia and reoxygenation in tumor parenchyma. Cancer Res. *56*, 5522–5528.

Klimberg, V.S., Suzannec Klimberg, V., and McClellan, J.L. (1996). Glutamine, cancer, and its therapy. The American Journal of Surgery *172*, 418–424.

Kowalczyk, M., Orłowski, M., Siermontowski, P., Mucha, D., Zinkiewicz, K., Kurpiewski, W., Zieliński, E., Kowalczyk, I., and Pedrycz, A. (2018). Occurrence of colorectal aberrant crypt foci depending on age and dietary patterns of patients. BMC Cancer *18*, 213.

Kruse, J.-P., and Gu, W. (2009). MSL2 promotes Mdm2-independent cytoplasmic localization of p53. J. Biol. Chem. *284*, 3250–3263.

Lafontaine, D.L.J. (2015). Noncoding RNAs in eukaryotic ribosome biogenesis and function. Nat. Struct. Mol. Biol. *22*, 11–19.

Lavin, M.F., and Gueven, N. (2006). The complexity of p53 stabilization and activation. Cell Death Differ. *13*, 941–950.

Leprivier, G., Remke, M., Rotblat, B., Dubuc, A., Mateo, A.-R.F., Kool, M., Agnihotri, S., El-Naggar, A., Yu, B., Somasekharan, S.P., et al. (2013). The eEF2 Kinase Confers Resistance to Nutrient Deprivation by Blocking Translation Elongation. Cell *153*, 1064–1079.

Levine, A.J. (2020). p53: 800 million years of evolution and 40 years of discovery. Nat. Rev. Cancer *20*, 471–480.

Lewis, E.J. (2015). PRIMA-1 as a cancer therapy restoring mutant p53: a review. Bioscience Horizons *8*, hzv006–hzv006.

Liu, G.Y., and Sabatini, D.M. (2020). mTOR at the nexus of nutrition, growth, ageing and disease. Nature Reviews Molecular Cell Biology *21*, 183–203.

Loree, J.M., Pereira, A.A.L., Lam, M., Willauer, A.N., Raghav, K., Dasari, A., Morris, V.K., Advani, S., Menter, D.G., Eng, C., et al. (2018). Classifying Colorectal Cancer by Tumor Location Rather than Sidedness Highlights a Continuum in Mutation Profiles and Consensus Molecular Subtypes. Clin. Cancer Res. *24*, 1062–1072.

Mamane, Y., Petroulakis, E., LeBacquer, O., and Sonenberg, N. (2006). mTOR, translation initiation and cancer. Oncogene *25*, 6416–6422.

May, P., and May, E. (1999). Twenty years of p53 research: structural and functional aspects of the p53 protein. Oncogene *18*, 7621–7636.

Mayer, C. (2004). mTOR-dependent activation of the transcription factor TIF-IA links rRNA synthesis to nutrient availability. Genes & Development *18*, 423–434.

Medema, J.P. (2013). Cancer stem cells: The challenges ahead. Nature Cell Biology *15*, 338–344.

Miller, R.A., Maloney, D.G., Warnke, R., and Levy, R. (1982). Treatment of B-Cell Lymphoma with Monoclonal Anti-Idiotype Antibody. New England Journal of Medicine *306*, 517–522.

Mullineux, S.-T., and Lafontaine, D.L.J. (2012). Mapping the cleavage sites on mammalian pre-rRNAs: where do we stand? Biochimie *94*, 1521–1532.

Muz, B., de la Puente, P., Azab, F., and Azab, A.K. (2015). The role of hypoxia in cancer progression, angiogenesis, metastasis, and resistance to therapy. Hypoxia (Auckl) *3*, 83–92.

Negi, S.S., and Brown, P. (2015). Transient rRNA synthesis inhibition with CX-5461 is sufficient to elicit growth arrest and cell death in acute lymphoblastic leukemia cells. Oncotarget *6*, 34846–34858.

Nicolas, E., Parisot, P., Pinto-Monteiro, C., de Walque, R., De Vleeschouwer, C., and Lafontaine, D.L.J. (2016). Involvement of human ribosomal proteins in nucleolar structure and p53-dependent nucleolar stress. Nat. Commun. *7*, 11390.

Ohh, M., Park, C.W., Ivan, M., Hoffman, M.A., Kim, T.Y., Huang, L.E., Pavletich, N., Chau, V., and Kaelin, W.G. (2000). Ubiquitination of hypoxia-inducible factor requires direct binding to the beta-domain of the von Hippel-Lindau protein. Nat. Cell Biol. *2*, 423–427.

Oliner, J.D., Saiki, A.Y., and Caenepeel, S. (2016). The Role of MDM2 Amplification and Overexpression in Tumorigenesis. Cold Spring Harb. Perspect. Med. *6*.

Osawa, T., and Shibuya, M. (2013). Targeting cancer cells resistant to hypoxia and nutrient starvation to improve anti-angiogeneic therapy. Cell Cycle *12*, 2519–2520.

Pàez-Ribes, M., Allen, E., Hudock, J., Takeda, T., Okuyama, H., Viñals, F., Inoue, M., Bergers, G., Hanahan, D., and Casanovas, O. (2009). Antiangiogenic therapy elicits malignant progression of tumors to increased local invasion and distant metastasis. Cancer Cell *15*, 220–231.

Pan, M., Reid, M.A., Lowman, X.H., Kulkarni, R.P., Tran, T.Q., Liu, X., Yang, Y., Hernandez-Davies, J.E., Rosales, K.K., Li, H., et al. (2016). Regional glutamine deficiency in tumours promotes dedifferentiation through inhibition of histone demethylation. Nat. Cell Biol. *18*, 1090–1101.

Pelletier, J., Thomas, G., and Volarević, S. (2018). Ribosome biogenesis in cancer: new players and therapeutic avenues. Nat. Rev. Cancer *18*, 51–63.

Peltonen, K., Colis, L., Liu, H., Trivedi, R., Moubarek, M.S., Moore, H.M., Bai, B., Rudek, M.A., Bieberich, C.J., and Laiho, M. (2014). A targeting modality for destruction of RNA polymerase I that possesses anticancer activity. Cancer Cell *25*, 77–90.

Pestov, D.G., Strezoska, Z., and Lau, L.F. (2001). Evidence of p53-Dependent Cross-Talk between Ribosome Biogenesis and the Cell Cycle: Effects of Nucleolar Protein Bop1 on G1/S Transition. Molecular and Cellular Biology *21*, 4246–4255.

Rebello, R.J., Kusnadi, E., Cameron, D.P., Pearson, H.B., Lesmana, A., Devlin, J.R., Drygin, D., Clark, A.K., Porter, L., Pedersen, J., et al. (2016). The Dual Inhibition of RNA Pol I Transcription and PIM Kinase as a New Therapeutic Approach to Treat Advanced Prostate Cancer. Clin. Cancer Res. *22*, 5539–5552.

Satoh, K., Yachida, S., Sugimoto, M., Oshima, M., Nakagawa, T., Akamoto, S., Tabata, S., Saitoh, K., Kato, K., Sato, S., et al. (2017). Global metabolic reprogramming of colorectal cancer occurs at adenoma stage and is induced by MYC. Proc. Natl. Acad. Sci. U. S. A. *114*,

E7697–E7706.

Scull, C.E., and Schneider, D.A. (2019). Coordinated Control of rRNA Processing by RNA Polymerase I. Trends Genet. *35*, 724–733.

Semenza, G.L. (2003). Targeting HIF-1 for cancer therapy. Nature Reviews Cancer *3*, 721–732.

Shangary, S., and Wang, S. (2009). Small-molecule inhibitors of the MDM2-p53 protein-protein interaction to reactivate p53 function: a novel approach for cancer therapy. Annu. Rev. Pharmacol. Toxicol. *49*, 223–241.

Sheen, J.-H., Zoncu, R., Kim, D., and Sabatini, D.M. (2011). Defective regulation of autophagy upon leucine deprivation reveals a targetable liability of human melanoma cells in vitro and in vivo. Cancer Cell *19*, 613–628.

Sherr, C.J. (2006). Divorcing ARF and p53: an unsettled case. Nat. Rev. Cancer *6*, 663–673.

Silvera, D., Formenti, S.C., and Schneider, R.J. (2010). Translational control in cancer. Nature Reviews Cancer *10*, 254–266.

Sloan, K.E., Bohnsack, M.T., and Watkins, N.J. (2013). The 5S RNP couples p53 homeostasis to ribosome biogenesis and nucleolar stress. Cell Rep. *5*, 237–247.

Sperka, T., Song, Z., Morita, Y., Nalapareddy, K., Guachalla, L.M., Lechel, A., Begus-Nahrmann, Y., Burkhalter, M.D., Mach, M., Schlaudraff, F., et al. (2011). Puma and p21 represent cooperating checkpoints limiting self-renewal and chromosomal instability of somatic stem cells in response to telomere dysfunction. Nat. Cell Biol. *14*, 73–79.

Stephen, A.G., Esposito, D., Bagni, R.K., and McCormick, F. (2014). Dragging ras back in the ring. Cancer Cell *25*, 272–281.

Thomlinson, R.H., and Gray, L.H. (1955). The histological structure of some human lung cancers and the possible implications for radiotherapy. Br. J. Cancer *9*, 539–549.

Thoreen, C.C., Chantranupong, L., Keys, H.R., Wang, T., Gray, N.S., and Sabatini, D.M. (2012). A unifying model for mTORC1-mediated regulation of mRNA translation. Nature *485*, 109–113.

Villar, V.H., Nguyen, T.L., Delcroix, V., Terés, S., Bouchecareilh, M., Salin, B., Bodineau, C., Vacher, P., Priault, M., Soubeyran, P., et al. (2017). mTORC1 inhibition in cancer cells protects from glutaminolysis-mediated apoptosis during nutrient limitation. Nat. Commun. *8*, 14124.

Vogelstein, B., Lane, D., and Levine, A.J. (2000). Surfing the p53 network. Nature *408*, 307–310.

Wade, M., Li, Y.-C., and Wahl, G.M. (2013). MDM2, MDMX and p53 in oncogenesis and cancer therapy. Nat. Rev. Cancer *13*, 83–96.

Wang, X., Regufe da Mota, S., Liu, R., Moore, C.E., Xie, J., Lanucara, F., Agarwala, U., Pyr Dit Ruys, S., Vertommen, D., Rider, M.H., et al. (2014). Eukaryotic elongation factor 2 kinase activity is controlled by multiple inputs from oncogenic signaling. Mol. Cell. Biol. *34*, 4088–4103.

Warburg, O. (1956). On the origin of cancer cells. Science *123*, 309–314.

Wise, D.R., and Thompson, C.B. (2010). Glutamine addiction: a new therapeutic target in cancer. Trends Biochem. Sci. *35*, 427–433.

Xu, H., Di Antonio, M., McKinney, S., Mathew, V., Ho, B., O'Neil, N.J., Santos, N.D., Silvester, J., Wei, V., Garcia, J., et al. (2017). CX-5461 is a DNA G-quadruplex stabilizer with selective lethality in BRCA1/2 deficient tumours. Nat. Commun. *8*, 14432.

Yang, K., Yang, J., and Yi, J. (2018). Nucleolar Stress: hallmarks, sensing mechanism and diseases. Cell Stress Chaperones *2*, 125–140.

Yang, Y., Han, Z., Li, X., Huang, A., Shi, J., and Gu, J. (2020). Epidemiology and risk factors of colorectal cancer in China. Chin. J. Cancer Res. *32*, 729–741.

Zhao, J., Yuan, X., Frödin, M., and Grummt, I. (2003). ERK-dependent phosphorylation of the transcription initiation factor TIF-IA is required for RNA polymerase I transcription and cell growth. Mol. Cell *11*, 405–413.

Zheng, L., Li, S., Boyer, T.G., and Lee, W.H. (2000). Lessons learned from BRCA1 and BRCA2. Oncogene *19*, 6159–6175.

(2017). Eukaryotic Elongation Factor 2 Kinase (eEF2K) in Cancer. Cancers *9*.